Available online at http://www.journalcra.com

International Journal of Current Research
Vol. 10, Issue, 03, pp.66290-66307, March, 2018

INTERNATIONAL JOURNAL OF CURRENT RESEARCH

ISSN: 0975-833X

RESEARCH ARTICLE

SPECTROSCOPIC (FT-IR, FT-RAMAN AND UV-VIS) STUDY, HOMO-LUMO, NBO AND MOLECULAR DOCKING ANALYSIS OF ALKYLATING AGENT: BIS-CHLOROETHYLNITROSOUREA

***,[1]Priyanka Singh, [2]Prabaharan, A., [1]Hilal Ahmad and [1]Islam, S. S.**

[1]Centre for Nanoscience and Nanotechnology, Jamia Millia Islamia, New Delhi-110025, India
[2]PG and Research Department of Physics, Periyar E.V.R College (Autonomous), Tiruchirappalli-620023, India

ARTICLE INFO

Article History:
Received 24th December, 2017
Received in revised form
20th January, 2018
Accepted 27th February, 2018
Published online 28th March, 2018

Key words:
Bis-chloroethylnitrosourea;
APT and Mulliken charges;
HOMO-LUMO; NBO;
AIM; Molecular Docking.

ABSTRACT

In this work, the structural and vibrational studies for the most stable conformer of the anticancer drug Bis-chloroethylnitrosourea (BCNU) or Carmustine have been carried out at the DFT/B3LYP/6-311++G(d,p) level using the Gaussian 09 software. It was predicted to exist predominantly in non-planar structure. The FT-IR (400–4000 cm^{-1}), FT-Raman spectra (300–4000 cm^{-1}) and UV-Vis spectra (200-400 nm) of BCNU were recorded and analyzed in light of the computed vibrational parameters using DFT (density functional theory) and the PEDs (Potential energy distribution) computed with the help of the GAR2PED software. The total and partial density of state and overlap population density of state diagrams analysis are presented for the BCNU molecule. Furthermore, molecular electrostatic potential, are performed. In addition to these, reduced density gradient of the BCNU molecule is performed and discussed. Stability of the molecule arising from hyper conjugative interactions, charge delocalization has been analyzed using natural bond orbital (NBO) analysis. The HOMO-LUMO energy gap reveals that the energy gap reflects the chemical activity of the molecule. The thermodynamic functions of the title compound have been performed by B3LYP/6-311+G(d,p). In addition, hyperpolarizability and molecular docking calculations were performed in order to find its role in non-linear optics and anticancer activity.

Citation: Priyanka Singh, Prabaharan, A., Hilal Ahmad and Islam, S. S., 2018. "Spectroscopic (ft-ir, ft-raman and uv-vis) study, homo-lumo, nbo and molecular docking analysis of alkylating agent: bis-chloroethylnitrosourea", *International Journal of Current Research*, 10, (03), 66290-66307.

INTRODUCTION

Bis-chloroethylnitrosourea (BCNU) or Carmustine (Fig.a) is a medication used mainly for chemotherapy and sometimes for immunosuppression before organ transplantation. BCNU is highly lipophilic and crosses the blood-brain barrier readily as well as is used to treat certain types of cancer. These include brain tumors, multiple myeloma, Hodgkin's disease, and non-Hodgkin's lymphoma (Ewend *et al.,* 2007). BCNU belongs to the family of therapeutic nitrosourea compounds used in cancer treatment. It is a nitrogen mustard β-chloro-nitrosourea compound used as an alkylating agent (antineoplastic agent). As a dialkylating agent, BCNU is able to form interstrand crosslinks in DNA, which prevents DNA replication and DNA transcription. This agent also carbamoylates proteins, including DNA repair enzymes, resulting in an enhanced cytotoxic effect. They are implanted under the skull during a surgery called a craniotomy. The disc allows for controlled release of BCNU in the extracellular fluid of the brain, thus eliminating the need for the encapsulated drug to cross the blood-brain barrier (Hopkins Medicine Magazine - In Spite of All Odds.). Hassani *et al.* (Hassaniet *et al.,* 2012) have presented the physicochemical properties of five anticancer drugs at the B3LYP/6-31G* level. Mansour *et al.* (Dalili Mansour *et al.,* 2014) have the studies the chemical interaction between the BCNU and carbon nanotubes (CNTs). Zhao *et al*. (2013) have investigated the mechanism for the formation of DNA ICLs (crosslinks) induced by BCNU. To the best of our knowledge, no work appears to have been reported on the complete vibrational assignment for the lowest energy conformer of BCNU molecule. Therefore, investigation of the complete vibrational spectrum of the BCNU molecule seems pertinent. In the present paper, we have investigated theoretically the optimized molecular geometries, and fundamental vibrational modes along with their IR intensities, Raman activities and depolarization ratios of the Raman bands of the most stable energy conformer at the B3LYP/6-311++G(d,p) level. We have also calculated the potential energy distributions (PEDs) for the normal modes of the BCNU molecule to make more reliable vibrational assignments. We have also investigated experimentally the IR and Raman spectra of BCNU, analysed these in light of the computational parameters and presented complete vibrational assignments of the observed spectra, and

Corresponding author:* **Priyanka Singh,
Centre for Nanoscience and Nanotechnology, Jamia Millia Islamia, New Delhi-110025, India.

correlated the calculated and observed frequencies. APT, Mulliken atomic charges as well as molecular docking were also computed. Change in the electron density (ED) in the antibonding orbitals and energies have been computed by the natural bond orbital (NBO) analysis method to provide definite proof of stabilization of the BCNU molecule.

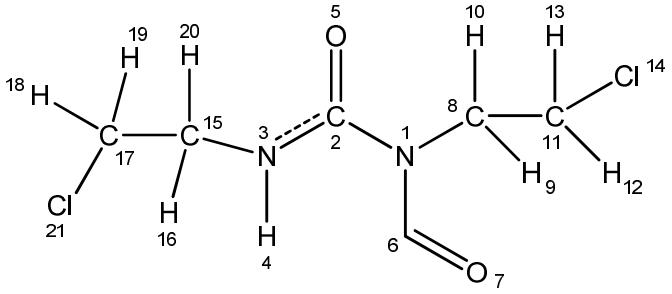

Fig.a. Molecular structure of BCNU molecule

Experimental techniques

The Bis-chloroethylnitrosourea (BCNU) molecule was provided from sigma-aldrich Company in the solid state with a stated purity of 99% and it was used as such without further purification. The sample was prepared using a KBr disc technique because of solid state. The infrared spectrum of the title molecule was recorded between 400-4000 cm^{-1} on a perkin-Elmer FT-IR System Spectrum BX spectrometer. The spectrum was recorded at room temperature, with a scanning speed of 10 $cm^{-1}min^{-1}$ and the spectral resolution of 4.0 cm^{-1}. FT- Raman spectrum of the molecule was recorded between 4000-300 cm^{-1} on a Bruker RFS 100/S FT-Raman instrument using 1064 nm excitation from an Nd:YAG laser. The UV-Vis absorption spectrum of the BCNU is examined in the range 200-400 nm using Shimadzu UV-2105 PC, UV-Vis recording Spectrometer, solved in ethanol.

Computational details

DFT calculations are important appliances for understanding the fundamental vibrational properties and the electronic structure of the compounds. To optimize the structure of BCNU, the following procedure was adopted. Initially, the structure of formamidyl was optimized. After this a NH_2 group was added to the sites of H and the structure was optimized. With this structure an N=O group was added and the structure with two possible conformers one with the lower energy was taken. Since the molecule has N=O group with two possible orientations and the structure was optimized. With this structure two methyl (CH3) groups was added at the position N1 and N_3 sites and structure with four possible orientations of the CH3 group were optimized. In the optimized structure, there are four possible orientations and the procedure outlined above is adopted to get minimum energy conformer. To this minimum energy conformer add two CH3 group was added to the H9, H10 and H11 sites and the resulting structure of the CH3 group were optimized and the procedure outlined above is adopted to get minimum energy conformer. With the minimum energy conformer two Cl is attached to the H12/21, H14/18 and H13/19 position. To this minimum energy conformer and the structure are optimized at the B3LYP/6-311++G** level. The geometry was fully optimized without any constraint. For the present study the lowest energy conformer is considered. The optimized molecular geometries, APT charges, Mulliken atomic charges and fundamental vibrational wavenumbers along with their corresponding intensities in IR spectrum, Raman activities and depolarization ratios of the Raman bands for the BCNU molecule were computed at the B3LYP/6-311++G(d,p) level using the Gaussian 09 (Frisch *et al.,* 2009) program package. The unscaled B3LYP/6-311++G (d, p) vibrational frequencies are generally larger than the experimental values. The computations have been performed using density functional theory (DFT) (Hohenberg and Kohn, 1964) at the B3LYP level. The B3LYP functional, consists of Becke's three-parameter (B3) hybrid exchange functional (Becke, 1993) was combined with Lee-Yang-Parr correlation functional (LYP) (Lee *et al.,* 1988) with the standard 6-311++g** basis set, accepted as a cost effective approach, for the computation of molecular structure, vibrational fundamental frequencies and energies of optimized structures. The basis set used as a Valence triple-zeta with the addition of diffuse and polarization functions for each atom in the molecule. In order to obtain the reasonable frequency matching, scale factors proposed by Rauhut and Pulay (Sundaraganesan *et al.,* 2015; Karabacak and Kurt, 2008) were employed. The assignments of all the normal modes of vibration have been made on the basis of the calculated potential energy distributions (PEDs). For the calculation of the PEDs the vibrational problem was set up in terms of internal coordinates using GAR2PED (Martin *et al.,* 1995) software.The observed IR and Raman frequencies corre sponding to the fundamental modes have been correlated to the calculated fundamental frequencies in light of the PEDs. The nature of the functional groups associating with the assigned normal modes is verified by the GaussView 05 (Frisch *et al.,* 2000) graphical animation program and also for the verification of the normal modes assignment. The electrostatic potential (ESP) surface and frontier molecular orbitals (FMOs) were calculated using B3LYP method of the DFT based on the optimized structure and visualized by the GaussView 05 software (Frisch *et al.,* 2000). Moreover, to calculate group contributions to the molecular orbitals and to prepare total density of states (TDOS or DOS), the partial density of states (PDOS) and overlap population density of states (OPDOS) spectra GaussSum2.2 (O'boyle *et al.,* 2008) was used.

The contribution of a group to a molecular orbital was calculated using Mulliken population analysis. The PDOS and OPDOS spectra were created by convoluting the molecular orbital information with Gaussian curves of unit height and an FWHM (full width at half maximum) of 0.3 eV. The changes of the heat capacity, entropy, and enthalpy of the title molecule were investigated for the different temperatures (from 100 K to 700 K) from the vibrational frequency calculations in gas phase. To calculate NLO properties (dipole moment, mean polarizability, and first static hyperpolarizability) of the molecule the finite field approach DFT were used. NBO 3.1 program as implemented in the Gaussian 09 package was used for NBO calculations at the DFT/B3LYP level. The NBO calculations were performed to understand varied second order interactions. These interactions were between the occupied orbitals and unoccupied orbitals, which are a measure of the intermolecular delocalization or hyper conjugation. The RDG is performed by Multiwfn, and plotted by VMD program, respectively. The molecular docking analysis was performed by the AUTODOCK 4.0.1 (version: 1.4.6) software and the ligand-protein binding pose was visualized by PyMOL molecular graphics system (version 1.7.4.5 Edu).

RESULTS AND DISCUSSION

Vibrational spectral analysis

The spectroscopic properties of BCNU have not yet been studied in detail to the best of our knowledge. The vibrational frequencies were obtained from the DFT/B3LYP method by using split valence basis sets along with diffuse and polarization function with 6-311++G (d,p). The vibrational wavenumbers, IR intensity, Raman activity, values were calculated for the most stable optimized structure of the BCNU molecule. The BCNU consist of 21 atoms, which has 57 vibrational degrees of freedom.

The 57 normal modes of BCNU have been assigned according to the detailed vibrations of the individual atoms. This molecule belongs to C_1 symmetry group and the proposed vibrational mode assignments (characterized by PED) are presented in Table 1. The experimental FT-IR and FT-Raman spectra are shown in Fig. 1 and Fig. 2 respectively. The calculated IR and Raman spectra are shown in Fig. 3 and Fig. 4 for comparative purpose where the calculated intensity is plotted against harmonic vibrational wavenumbers. The computed harmonic frequencies were scaled factors in order to improve the agreement with the experimental results. In our study, we have followed two different scaling factors such as

Table 1. Calculated and observed vibrational frequencies and assignments for the BCNU molecule

S.No.	Calculated		Observed		[b]Vibrational assignments along with PED (%)
	Unscaled freq. (IR, Raman) depolarization ratio	Scaled freq.[a]	IR	Raman	
1	12(0.93,0.49)0.73	12	-	-	τHNCC(70)
2	30(0.28,0.46)0.70	28	-	-	τHCNC(43)+τHCNN(25)
3	47(0.22,1.10)0.73	45	-	-	τCNCC(46)+τHCNC(12)+τHCNN(11)
4	57(3.33,1.13)0.70	54	-	-	τHNCC(73)
5	74(2.15,0.58)0.73	71	-	-	τHCNC(43)+τHCCH(18)
6	103(3.36,0.13)0.66	99	-	-	τHCCH(25) + τHCNN(29)
7	135(11.39,0.58)0.34	130	-	-	τHCNC(52)
8	184(4.53,1.18)0.66	177	-	-	δ_{out}CCN(11)+δ_{in}CCCl(11)+τHCCCl(21)
9	233(3.71,0.93)0.38	223	-	-	δ_{in}CCCl(44)
10	237(11,0.86)0.52	228	-	-	δ_{in}HCC(17)
11	271(3.92,2.52)0.19	260	-	-	δ_{in}CCN(30)
12	347(11.78,0.19)0.70	333	-	-	δ_{out}CNC(60)
13	372(25.78,0.55)0.23	358	-	-	τHCCH(20)+τHCNN(20)+δ_{out}HCN(10)
14	410(2.97,2.12)0.16	394	-	-	τHCCCl(10)+τHCNC(11)
15	465(5.09,2.91)0.68	447	-	-	δ_{in}HCC(35)+δ_{out}CCN(10)
16	498(2.65,4.04)0.21	478	-	-	δ_{in}CCN(18)+ν_{ss}NC(35)+δ_{in}CNN(11)
17	544(17.20,0.64)0.39	523	-	505	δ_{in}HCC(35)+δ_{in}HCN(10)
18	545(87.97,0.23)0.36	524	-	-	τHNCN(82)
19	651(29.53,11.10)0.24	626	604	549	ν_{ss}ClC(77)
20	737(24.87,12.44)0.20	708	-	653	δ_{in}HCN(26)+ν_{ss}ClC(25)
21	757(25.74,10.56)0.43	728	-	697	τHCCH(11)+ν_{ss}ClC(38)
22	765(27.37,1.38)0.52	735	-	-	τHCNN(59)
23	800(37.49,4.43)0.06	769	-	-	δ_{in}HCC(37)+δ_{in}HCC(10)
24	854(58.36,9.18)0.08	821	-	808	δ_{in}CNN(18)+τHCCH(20)
25	878(4.34,6.81)0.29	844	-	-	τHCCH(12)+ν_{ss}CC(44)
26	964(90.93,3.01)0.35	927	-	-	ν_{ss}CC(52)
27	984(72.55,4.11)0.65	946	-	-	τHCCH(22)+ν_{ass}CC(39)
28	1034(60.41,1.34)0.37	993	-	-	ν_{ass}CC(11)+ν_{ass}NN(15)+δ_{in}HCC(27)
29	1049(0.71,4.91)0.16	1008	-	-	ν_{ss}CC(79)
30	1083(67.49,1.77)0.41	1041	1016	-	ν_{ss}NN(28)+δ_{in}HCC(16)
31	1106(60.76,1.80)0.68	1063		-	τHCNN(13)+ν_{ass}CC(18)+δ_{out}HCN(17)
32	1179(71.56,3.33)0.13	1133		-	ν_{ss}NC(53)+δ_{out}HNC(13)
33	1209(0.57,4.67)0.72	1162	1171	-	δ_{out}HNC(62)
34	1263(15.22,4.40)0.44	1213	-	-	δ_{out}HCN(45)+ν_{ss}CC(10)
35	1287(14.25,8.58)0.40	1237	-	-	δ_{in}HCC(51)
36	1297(44.29,0.93)0.54	1246	-	-	δ_{in}HCCl(81)
37	1312(84.44,4.74)0.23	1261	-	-	ν_{ass}NC(15)+δ_{in}HNC(10)
38	1347(21.68,3.38)0.67	1295	-	-	τHNCH(49)
39	1368(60.68,15.48)0.60	1315	1304	-	δ_{in}HCN(58)
40	1395(13.65,1.99)0.20	1341	-	-	δ_{in}HCN(63)
41	1408(7.88,2.06)0.60	1353	-	-	δ_{out}HCN(59)
42	1462(14.17,18.05)0.47	1405	-	-	δ_{in}HCH(88)
43	1467(18.11,8.89)0.73	1410	-	-	δ_{in}HCH(86)
44	1477(8.26,8.11)0.68	1420	1415	-	δ_{in}HCH(89)
45	1485(7.16,6.14)0.59	1428	-	-	δ_{in}HCH(92)
46	1548(521.07,5.37)0.53	1488	1444	1433	δ_{out}HNC(51)
47	1592(198.11,25.77)0.38	1530	-	1498	ν_{ss}ON(79)
48	1777(284.34,22.075)0.16	1707	1763	1698	ν_{ss}OC(75)
49	3062(19.31,128.25)0.06	2942	-	-	ν_{ss}CH(99)
50	3090(9.94,139.28)0.10	2969	-	-	ν_{ss}CH(93)
51	3092(0.59,138.38)0.03	2972	-	-	ν_{ss}CH(97)
52	3103(11.60,1.07)0.73	2982	-	-	ν_{ass}CH(97)
53	3110(4.05,65.67)0.60	2988	-	-	ν_{ass}CH(92)
54	3151(1.15,58.78)0.72	3028	-	-	ν_{ass}CH(96)
55	3154(5.80,54.69)0.68	3031	-	-	ν_{ass}CH(97)
56	3171(0.01,1.64)0.21	3047	-	-	ν_{ass}CH(98)
57	3609(61.66,50.08)0.10	3468	-	-	ν_{ss}NH(100)

[b]The abbreviations are – ν_{ss} - symmetrical stretching, ν_{ass} - asymmetrical stretching, δ_{in} - in-plane bending, δ_{out} - out-of-plane bending, τ – torsion. [a]Calculated wave numbers below 1000 cm^{-1} were scaled by the scale factor 0.9786 and those above 1000 cm^{-1} by the scale factor 0.9550 for larger wave numbers.

0.983 up to 1700 cm^{-1} and 0.958 for greater than 1700 cm^{-1} (Sundaraganesan *et al.,* 2015; Karabacak and Kurt, 2008). The aim of this part of this study is the assignment of the vibrational absorptions to make a comparison with the related molecules and also with the results obtained from the theoretical calculations. There are some strong frequencies useful to characterize in the infrared and Raman spectra. It is worth mentioning that, for our molecule, the stretching vibrational modes are CO, NN, CN, CH, CC, CCl, NO and NH. However, there is great mixing of the CH_2 vibrational modes. The descriptions of the modes are very complex because of the low symmetry of the studied molecule. Especially, in plane modes and out of plane modes are the most difficult to assign due to mixing with the CH_2 modes and also with the substituent modes. Therefore, we discussed here had strong frequencies and lower frequencies of the calculated modes and had experimental values.

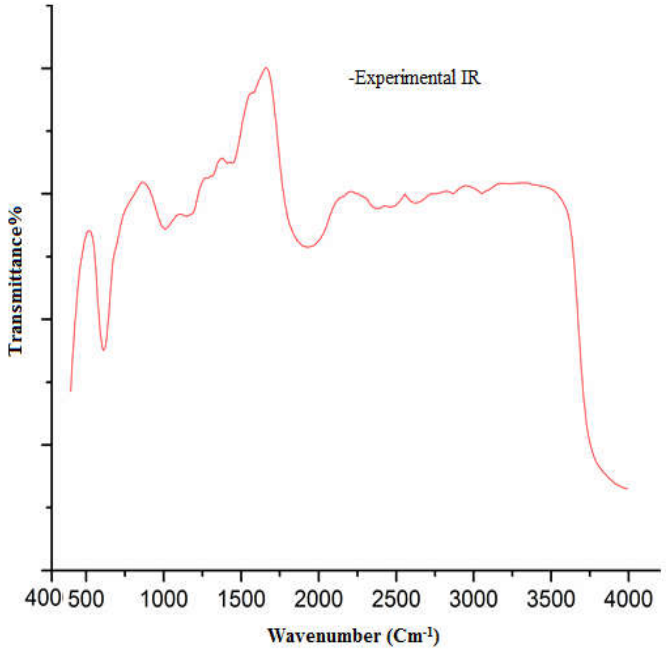

Fig. 1. The experimental infrared spectra of BCNU

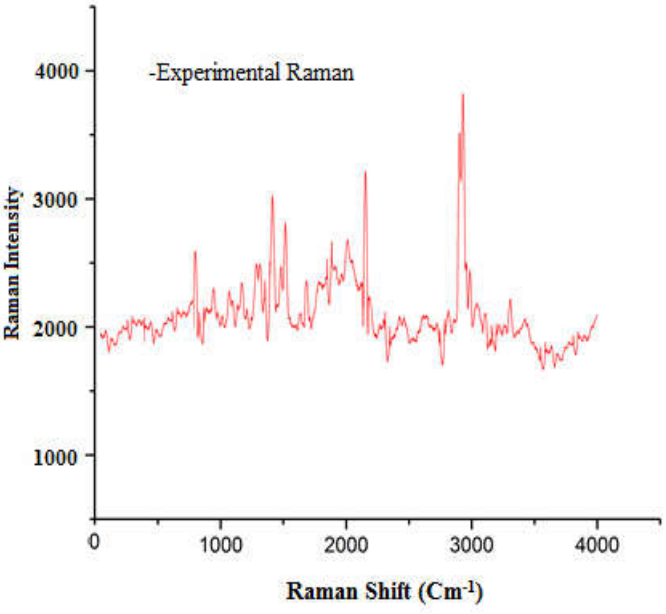

Fig. 2. The experimental Raman spectra of BCNU

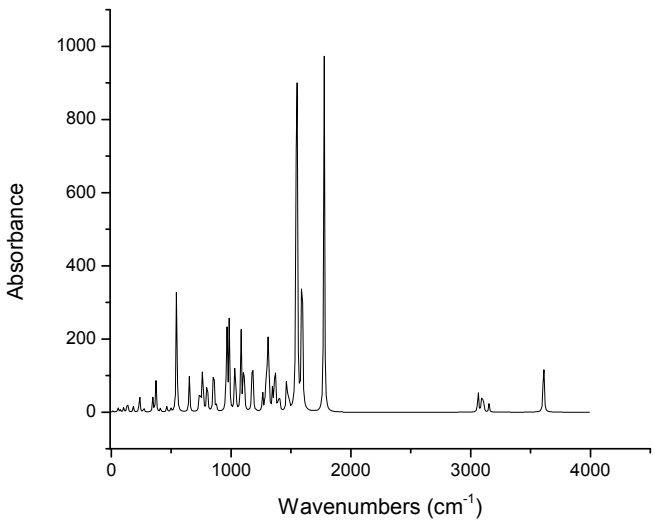

Fig. 3. The calculated infrared spectra of BCNU

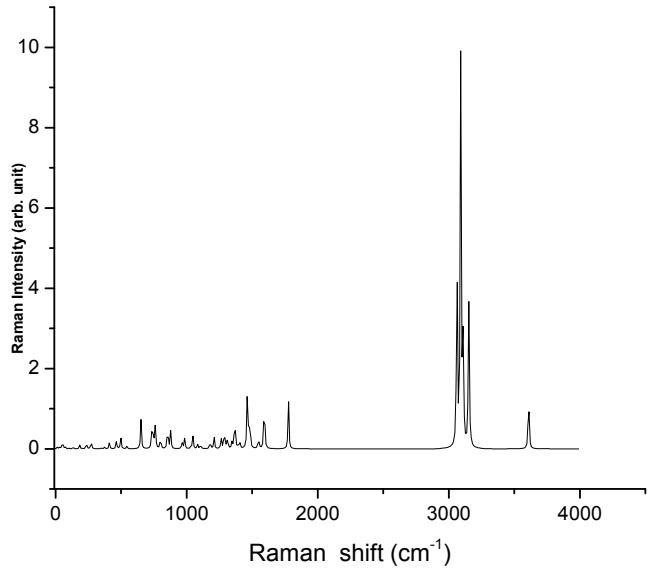

Fig. 4. The calculated Raman spectra of BCNU

CH_2 modes (24 modes)

The CH_2 group has six normal modes of vibration as: an anti-symmetric stretching mode-ν_{as} (CH_2), a symmetric stretching mode-ν_s(CH_2), a scissoring mode-σ(CH_2), a wagging mode-ω(CH_2), a torsional mode-τ(CH_2) and a rocking mode-ρ(CH_2). The BCNU molecule has four CH_2 groups in the eight, eleven, fifteen and seventeen positions. The CH_2 anti-symmetry and symmetry stretching mode (ν_{56},ν_{55},ν_{54}, ν_{53},ν_{52},ν_{51}, ν_{50} and ν_{49}) do not couple with any other modes, except the anti-symmetry stretching mode ν_{56} strongly couples with the ν_{54} mode while the ν_{54} mode strongly couples with the ν_{56} mode. The CH_2 symmetry stretching mode ν_{52} strongly couples with the CH_2 symmetry stretching ν_{51} mode while CH_2 symmetry stretching mode ν_{51} strongly couples with the CH_2 symmetry stretching ν_{52} mode. The CH_2 anti-symmetry and symmetry stretching modes are showed 100% contribution according to PED and the assignment of Gauss view program. In our present study, the frequency observed at 1415 cm^{-1} in the FT-IR spectrum are assigned to CH_2 scissoring mode shows good agreement with computed wavenumbers at 1485 cm^{-1}, 1477 cm^{-1}, 1467 cm^{-1} and 1462 cm^{-1} (ν_{45-42}) respectively.

Table 2. Calculated optimized parameter values of the BCNU molecule

Bond length (Å)	B3LYP	Bond angle (°)	B3LYP	Dihedral angle (°)	B3LYP
$r(N_1-C_2)$	1.438	$\alpha(C_2-N_1-N_6)$	117.574	$\delta(N_6-N_1-C_2-N_3)$	0.824
$r(N_1-N_6)$	1.353	$\alpha(C_2-N_1-C_8)$	120.094	$\delta(N_6-N_1-C_2-O_5)$	-178.331
$r(N_1-C_8)$	1.469	$\alpha(N_6-N_1-C_8)$	122.326	$\delta(C_8-N_1-C_2-N_3)$	-178.280
$r(C_2-N_3)$	1.353	$\alpha(N_1-C_2-N_3)$	115.066	$\delta(C_8-N_1-C_2-O_5)$	2.566
$r(C_2=O_5)$	1.215	$\alpha(N_1-C_2-O_5)$	119.334	$\delta(C_2-N_1-N_6-O_7)$	178.548
$r(N_3-H_4)$	1.010	$\alpha(N_3-C_2-O_5)$	125.594	$\delta(C_8-N_1-N_6-O_7)$	-2.370
$r(N_3-C_{15})$	1.454	$\alpha(C_2-N_3-C_{15})$	118.443	$\delta(C_2-N_1-C_8-H_9)$	146.429
$r(N_6=O_7)$	1.211	$\alpha(C_4-N_3-C_{15})$	121.139	$\delta(C_2-N_1-C_8-H_{10})$	28.047
$r(C_8-H_9)$	1.090	$\alpha(H_4-N_3-H_5)$	120.010	$\delta(C_2-N_1-C_8-C_{11})$	-92.838
$r(C_8-H_{10})$	1.087	$\alpha(N_1-N_6-O_7)$	115.638	$\delta(N_6-N_1-C_8-H_9)$	-32.630
$r(C_8-C_{11})$	1.527	$\alpha(N_1-C_8-H_9)$	107.236	$\delta(N_6-N_1-C_8-H_{10})$	-151.012
$r(C_{11}-H_{12})$	1.088	$\alpha(N_1-C_8-H_{10})$	107.214	$\delta(N_6-N_1-C_8-C_{11})$	88.10
$r(C_{11}-H_{13})$	1.088	$\alpha(N_1-C_8-C_{11})$	111.143	$\delta(N_1-C_2-N_3-H_4)$	5.675
$r(C_{11}-Cl_{14})$	1.811	$\alpha(H_9-C_8-H_{10})$	110.238	$\delta(N_1-C_2-N_3-C_{15})$	178.341
$r(C_{15}-H_{16})$	1.092	$\alpha(H_9-C_8-C_{11})$	110.387	$\delta(O_5-C_2-N_3-H_4)$	-175.232
$r(C_{15}-C_{17})$	1.5224	$\alpha(H_{10}-C_8-C_{11})$	110.519	$\delta(O_5-C_2-N_3-C_{15})$	-2.566
$r(C_{15}-H_{20})$	1.092	$\alpha(C_8-C_{11}-H_{12})$	111.656	$\delta(C_2-N_3-C_{15}-H_{16})$	146.145
$r(C_{17}-H_{18})$	1.089	$\alpha(C_8-C_{11}-H_{13})$	111.251	$\delta(C_1-N_3-C_{15}-C_{17})$	-90.918
$r(C_{17}-H_{19})$	1.088	$\alpha(C_8-C_{11}-H_{14})$	109.624	$\delta(C_1-N_3-C_{15}-H_{20})$	29.038
$r(C_{17}-Cl_{21})$	1.818	$\alpha(H_{12}-C_{11}-H_{13})$	110.478	$\delta(H_4-N_3-C_{15}-H_{16})$	-41.302
		$\alpha(H_{12}-C_{11}-H_{14})$	106.774	$\delta(H_4-N_3-C_{15}-C_{17})$	81.634
		$\alpha(H_{13}-C_{11}-H_{14})$	106.839	$\delta(H_4-N_3-C_{15}-H_{20})$	-158.410
		$\alpha(N_3-C_{15}-H_{16})$	108.383	$\delta(N_1-C_8-C_{11}-H_{12})$	-61.220
		$\alpha(N_3-C_{15}-C_{17})$	114.014	$\delta(N_1-C_8-C_{11}-H_{13})$	62.719
		$\alpha(N_3-C_{15}-H_{20})$	107.914	$\delta(N_1-C_8-C_{11}-Cl_{14})$	-179.334
		$\alpha(H_{16}-C_{15}-C_{17})$	110.058	$\delta(H_9-C_8-C_{11}-H_{12})$	57.637
		$\alpha(H_{16}-C_{15}-H_{20})$	108.327	$\delta(H_9-C_8-C_{11}-H_{13})$	-178.422
		$\alpha(C_{17}-C_{15}-H_{20})$	107.989	$\delta(H_9-C_8-C_{11}-Cl_{14})$	-60.476
		$\alpha(C_{15}-C_{17}-H_{18})$	110.609	$\delta(H_{10}-C_8-C_{11}-H_{12})$	179.855
		$\alpha(C_{15}-C_{17}-H_{19})$	111.583	$\delta(H_{10}-C_8-C_{11}-H_{13})$	-56.206
		$\alpha(C_{15}-C_{17}-H_{21})$	111.568	$\delta(H_{10}-C_8-C_{11}-Cl_{14})$	61.741
		$\alpha(H_{18}-C_{17}-H_{19})$	109.792	$\delta(N_3-C_{15}-C_{17}-H_{18})$	177.184
		$\alpha(H_{18}-C_{17}-Cl_{21})$	106.451	$\delta(N_3-C_{15}-C_{17}-H_{19})$	54.650
		$\alpha(H_{19}-C_{17}-Cl_{21})$	106.638	$\delta(N_3-C_{15}-C_{17}-Cl_{21})$	-64.523
				$\delta(H_{16}-C_{15}-C_{17}-H_{18})$	-60.797
				$\delta(H_{16}-C_{15}-C_{17}-H_{19}$	176.670
				$\delta(H_{16}-C_{15}-C_{17}-Cl_{21})$	57.496
				$\delta(H_{20}-C_{15}-C_{17}-H_{18})$	57.271
				$\delta(H_{20}-C_{15}-C_{17}-H_{19})$	-65.263
				$\delta(H_{20}-C_{15}-C_{17}-Cl_{21})$	175.564

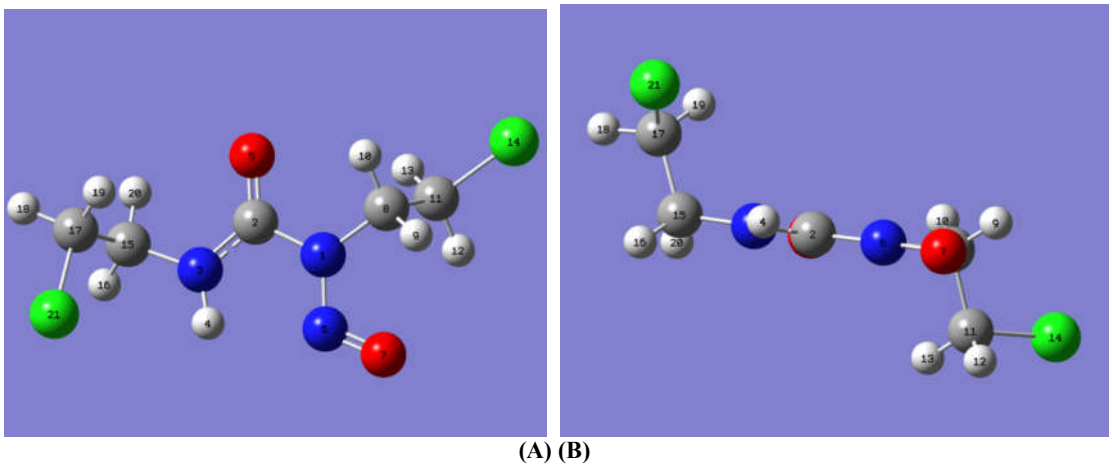

(A) (B)

Fig. 5. (A) Front (B) lateral view of optimized structures of BCNU

The wavenumbers for the wagging vibrations ($\nu_{41, 40, 36, 35}$) are falling in the region 1400-1280 cm^{-1} by B3LYP/6-311++g** method. The CH_2 torsions vibrations ($\nu_{39, 38, 34, 33}$) is expected in the range 1360-1200 cm^{-1} and for the rocking ($\nu_{28, 27, 23, 20}$) in the range 1030-730 cm^{-1}. In BCNU molecule, the torsion and rocking modes are calculated at 1368 cm^{-1}, 1209 cm^{-1} and 737 cm^{-1} shows good agreement with the recorded FT-IR band at 1304 cm^{-1} ν_{39} and 1171 cm^{-1} ν_{37} and FT-Raman spectrum at 653 cm^{-1} $\nu_{20.}$

C=O/ N=O modes (6 modes)

For the assignment of C=O group frequencies, basically three fundamentals can be associated to each C=O group namely, C=O stretching mode ν_{48}, C=O in-plane bending mode ν_{13} and

C=O out-of-plane bending mode ν_{22}. CH_2, C-Cl, N-H, N=O and C=O are the main functional groups associated with this molecule. This most of the characteristic features of the carboxylic group are observed usually 1750-1600 cm^{-1} region. The C=O bands being highly polar show intense peak both in the FT-IR and FT-Raman spectra. The C=O stretching vibration is calculated at 1707 cm^{-1} with matches with the observed peak at 1763 cm^{-1} in the FT-IR and at 1698 cm^{-1} in the FT-Raman spectrum. The in-plane/out-of-plane bending modes are calculated 372/765 cm^{-1} with the PED contribution 20% and 50% respectively. The N=O group frequencies are three fundamentals can be associated to each N=O group namely, N=O stretching mode ν_{47}, N=O angle bending modeν_{24} and N=O in-plane bending mode ν_{14}. The N=O starching vibrations are computed 1592 cm^{-1} by B3LYP method and observed 1498 cm^{-1} in the FT-Raman with the PED contribution 79%. The identification of wavenumber for N=O in-plane/angle bending mode in the side chain is rather difficult since there are problems in differentiating those wavenumbers from others. The N=O angle/in-plane bending modes are assigned to the wavenumbers 854 cm^{-1} (808 cm^{-1} in the FT-Raman spectrum) and 410 cm^{-1} have PED 20% and 11% respectively.

C-Cl/N-H modes (8 modes)

The C-Cl stretching modes ($\nu_{21,\ 19}$) are calculated at 757 cm^{-1} and 651 cm^{-1} with the PED contribution 38% and 77 %. The experimental values are in very god coherent, observed at 604 cm^{-1} (ν_{19}) in FT-IR spectrum whereas 697 cm^{-1} (ν_{21}) and 549 cm^{-1} (ν_{19}) in FT-Raman spectrum respectively. The C-C in-plane (ν_{11}) and out-of-plane ($\nu_{15,\ 12}$) vibrations were calculated in low wavenumber region which is presented in Table 1. The calculated N-H stretching vibrations (ν_{57}) wavenumber are found to be at 3609 cm^{-1} by using B3LYP/6-311++G** method. As expected this mode is pure stretching mode as it is evident from PED column, it is almost contributing 100%. The N-H in- plane bending vibration (ν_{46}) was also predicted at 1548 cm^{-1} with 51% PED contribution. The corresponding bands are observed at 144 cm^{-1} in FT-IR spectrum and 1433 cm^{-1} in FT-Raman spectrum was assigned to N-H in-plane bending mode. The N-H out-of-plane bending vibrational wavenumber was calculated at 5 45 cm^{-1} (ν_{18}) and they are almost pure modes and not much affected by the vibrations of other substituents.

4.1.4. C-C/C-N/N-N modes (7 stretching modes)

The bands at 1106 cm^{-1} and 1049 cm^{-1} have been assigned to the C-C stretching modes ($\nu_{31,\ 29}$). The PED corresponding to this (ν_{29}) vibration suggests that it is pure modes and exactly contributing to 79% whereas the ν_{31} vibration are not pure mode as it is evident from the last column of Table 1. The C-C stretching vibrations generally showed pure modes according to their PED and some of these modes are contaminated other vibrations. An identification of C-N stretching vibration is a difficult task due to the coupling of several other vibrational modes. The C-N/N-C stretching wavenumbers ($\nu_{37,\ 32,\ 30,\ 25}$) were computed by B3LYP method in the region 1300-870 cm^{-1}. We also identified according to PED calculations shows that the C-N/N-C stretching modes are nearly pure modes. In our calculations, the N-N stretching mode (ν_{26}) was calculated at 964 cm^{-1}. From Table 1, it can be shown that the PED calculations give contaminated with the some torsion of HCCH modes.

Bending, torsion and other modes (12 modes)

The calculated wavenumbers at 544, 237 and 233 cm^{-1} ($\nu_{17,\ 10,\ 9}$) were assigned to HCCN in-plane deformation modes and they are not pure mode and much affected by the other modes. The (ν_{17}) in-plane deformation were assigned at 505 cm^{-1} in FT-Raman spectrum with 35% PED contribution for BCNU molecule. The twisting vibrational wavenumbers ($\nu_{8\text{-}1}$) were calculated in low wavenumber region, which is presented in Table 1.

Geometrical parameters analysis

The most relevant structural parameters, bond lengths, bond angles and dihedral angle of BCNU determined by density functional theoretical calculations B3LYP method with 6-311++G** basis set (Table 2) using Gaussian 09 program package. The atom numbering of the BCNU molecule used in this paper is reported in Fig. 5. To the best of knowledge experimental data on the geometrical structure of the title molecule is not available till now in the literature. The magnitude of the bond lengths N_1-N_6 and N_3-H_4 are found to be 1.353 A° and 1.010 A° respectively. Bond length C=O and N=O indicates that the both C=O and N=O possess double bond character. No major changes are found in the bond lengths N-C, C-H, C-C and C-Cl from their corresponding usual bond lengths. The optimized bond angles C-N-C observed in the range of 118.443°-121.391°. Similarly, C-C-H is computed from 107.989° to 111.656°. The dihedral angles δ(C8-N1-C2-O5)/δ(C8-N1-C2-N3) are found to be 2.566° and -178.280° respectively.

APT and Mulliken atomic charges

Atomic polarizability tensor (APT) charge (Ferreira *et al.,* 1992) is interpreted as the sum of the charge tensor and charge flux tensor, leading to a charge-charge flux model. Mulliken atomic charge (Rastogi *et al.,* 2007) calculation has an important role in the application of quantum chemical calculation to molecular system because atomic charges affect dipole moment, polarizability, electronic structure and much more properties of molecular systems. APT and Mulliken atomic charge (in unit of e) at various sites of BCNU have been calculated using B3LYP/6-311++G** basis set and are listed in Table 3. The N atom (N_1 and N_3) possess negative APT charge with magnitudes 0.784 and 0.814 a.u. respectively whereas in Mulliken atomic charge N_1 atom possess positive charge (0.265 a.u.) while N_3 atom possess negative charge (0.320 a.u.). The C_2 atom which is directly attached to the O atom is more positive APT charge. From Table 3, it could be seen that the remaining carbon atoms (C_8, C_{11}, C_{15} and C_{17}) possess positive charge with magnitudes 0.231, 0.365, 0.360 and 0.324 a.u. respectively. The entire C atom (C_4, C_8, C_{11}, C_{15} and C_{17}) possess negatively Mulliken atomic charge which magnitudes 0.189, 0.207, 0.636, 0.227 and 0.341 a.u. respectively. The two oxygen O atoms (O_5 and O_7) possess negative APT and Mulliken atomic charges with magnitudes 0.807/0.317 and 0.575/0.039 a.u. respectively. The charge distribution of the title molecule shows all the hydrogen atoms are positively Mulliken atomic charge. In APT atomic charge, there are 9 hydrogen atom in the molecule in which 5 hydrogen atoms (H_{12}, H_{13}, H_{16}, H_{18} and H_{19}) possess negative

charge with magnitudes 0.005, 0.004, 0.010, 0.024 and 0.002 a.u. respectively whereas the remaining 4 hydrogen atoms (H_4, H_9, H_{10} and H_{20}) have positive charge as 0.247, 0.025, 0.055 and 0.022 a.u. respectively. It can be seen that the H_4 atom which is directly attached to the N atom bear positive and highest APT charge. It could be seen that the Cl atoms (Cl_{14} and Cl_{21}) which are directly attached to carbon atom bear negative APT charge while in the case of Mulliken atomic charge possess positive charge with magnitudes 0.205 and 0.031 a.u. respectively.

Table 3. Calculated APT charges and Mulliken atomic charges of the BCNU molecule

Atoms	APT atomic charges[a] (B3LYP/6-311++G**)	Mulliken atomic charges[a] (B3LYP/6-311++G**)
N_1	-0.784	0.265
C_2	1.462	-0.189
N_3	-0.814	-0.191
H_4	0.247	0.320
O_5	-0.807	-0.317
N_6	0.598	-0.305
O_7	-0.575	-0.039
C_8	0.231	-0.207
H_9	0.025	0.196
H_{10}	0.055	0.181
C_{11}	0.365	-0.636
H_{12}	-0.005	0.208
H_{13}	-0.004	0.237
Cl_{14}	-0.339	0.205
C_{15}	0.360	-0.227
H_{16}	-0.010	0.189
C_{17}	0.324	-0.341
H_{18}	-0.024	0.196
H_{19}	-0.002	0.230
H_{20}	0.022	0.194
Cl_{21}	-0.326	0.031

[a] In unit of e.

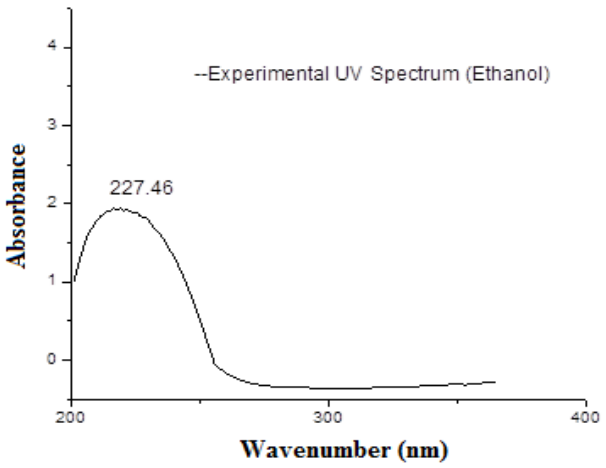

Fig. 6. The experimental UV-Vis spectrum of BCNU for ethanol

Electronic properties

Frontier molecular orbital (FMO_S) analysis

The most important orbitals in a molecule for reactivity are the two frontier molecular orbitals (FMOs), called highest occupied molecular orbital (HOMO) and lowest unoccupied molecular orbital (LUMO). The HOMO and LUMO orbital determine the way the molecule interacts with other species and very useful for electric and optical properties as well as UV-visible spectra and also the main orbital taking part in the chemical reaction. The HOMO energy represents the ability of electron giving, and LUMO represents the ability of electron accepting. The analysis of the wavefunction indicates that the electron absorption corresponds to the transition from the

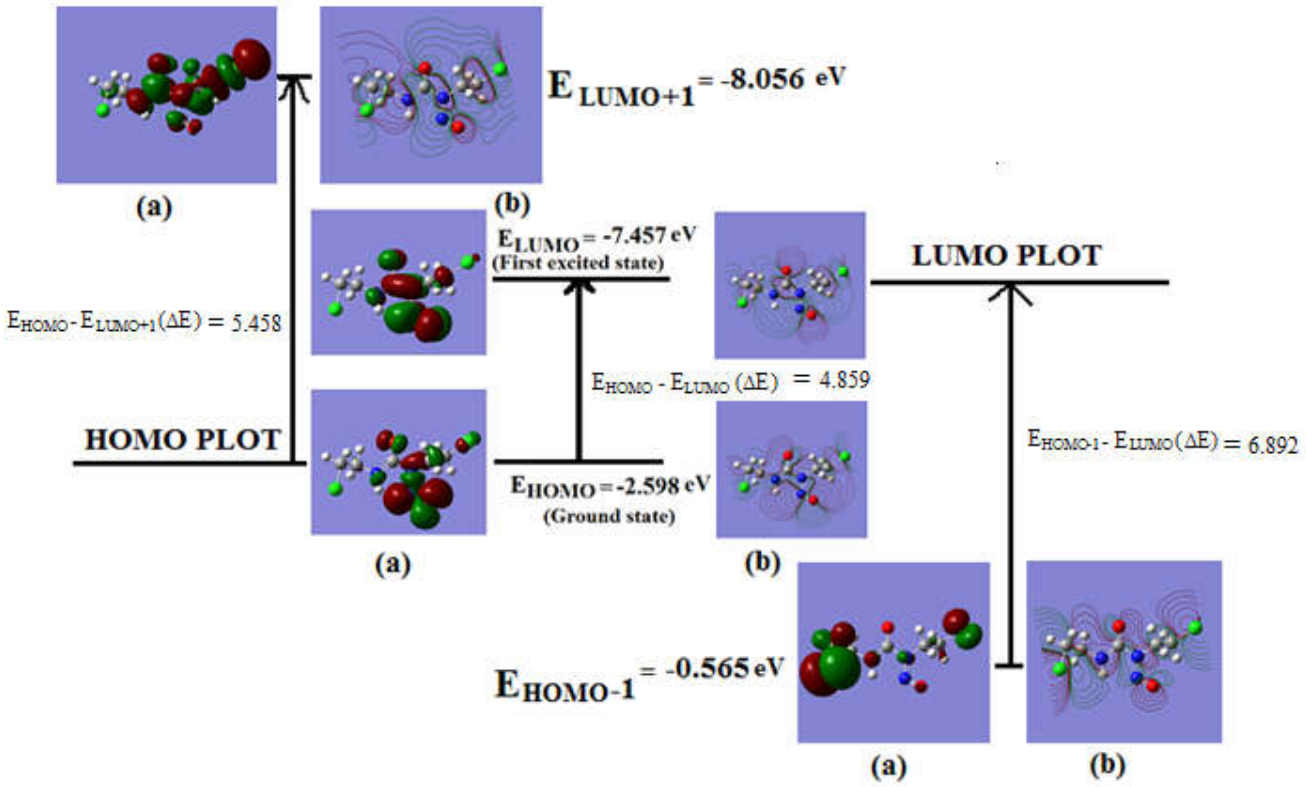

Fig. 7. (a) Frontier molecular orbital and (b) Contour map of FMO of BCNU molecule

ground to the first excited state and is mainly described by one-electron excitation from highest occupied molecular orbital (HOMO) and lowest unoccupied molecular orbital (LUMO). The energy of the HOMO is directly related to the ionization potential, while LUMO energy is directly related to the electron affinity (Gunasekaran *et al.,* 2008). The energy gap between HOMO and LUMO represents the molecular chemical stability. The energy gap (ΔE) is largely responsible for the chemical and spectroscopic properties of the molecules. This is also used by the frontier electron density for predicting the most reactive position in π-electron system and also explains several types of reaction in conjugate system (Fukui *et al.,* 1952). The conjugate molecules are represented by a small HOMO-LUMO energy gap (ΔE), which is the result of a significant degree of intra-molecular charge transfer (ICT) from end capping electron donor group to the efficient electron-acceptor group through π-conjugated path (Choi and Kertesz, 1997). Fig. 7, shows the surface of frontier molecular orbital (HOMO-1, HOMO, LUMO, LUMO+1) are drawn and the represents the bonding scheme of BCNU molecule as well as the picture of contour maps of FMOs. The HOMO and LUMO energy are calculated by B3LYP/6-311++G(d,p) method and listed in Table 4.

Table 4. The calculated energies value of BCNU molecule using by B3LYP/6-311++G(d,p)

Parameters	BCNU[a]
E_{HOMO}	-2.598
E_{HOMO-1}	-0.565
E_{LUMO}	-7.457
E_{LUMO+1}	-8.056
E_{HOMO} - E_{LUMO} (ΔE)	4.859
E_{HOMO} - E_{LUMO+1} (ΔE)	5.458
E_{HOMO-1} - E_{LUMO} (ΔE)	6.892
Chemical Hardness (η)	-1.131
Chemical Softness(S)	-0.885
Electronegativity(χ)	6.327
Chemical Potential(μ)	-6.327
Electrophilicity index(ω)	-35.404

[a] All the parameters are measured in eV .

The energy gap (ΔE), the difference between E_{HOMO}-E_{LUMO}, E_{HOMO}-E_{LUMO+1}, E_{HOMO-1}-E_{LUMO}. The energy gap between HOMO and LUMO orbital which is a critical parameter in determining molecular electron transport properties because which it is a measure of electron conductivity. The most important energy gap (E_{HOMO}-E_{LUMO}, E_{HOMO}-E_{LUMO+1}, E_{HOMO-1}-E_{LUMO}) were calculated at 4.859, 5.458 and 6.892 eV for the BCNU molecule. The HOMO of BCNU molecule is π- orbital while the LUMO is π*-orbital. The transition state of π-π* type is observed with regard to the molecular orbital theory. Also, the contributions of these transitions were computed Gauss Sum2.2 program. The red and green colors are positive phase and negative phase, respectively. The HOMO and LUMO are placed nearly similarly nodes. However the HOMO-1 and LUMO+1 have no similar nodes. The HOMO and LUMO are mainly localized in nitrosourea part of this molecule. Moreover the energy gap explains the eventual charge transfer interaction taking place within the molecule. The most important energy and the energy gap of the BCNU molecule are given in Table 4.

Reactivity descriptors

Chemical reactivity descriptors of compounds such as hardness(η), softness(S), electronegativity(χ), chemical potential(μ) and Electrophilicity index(ω) as well as local reactivity have been defined (20-24). The contour HOMO-LUMO diagram is in accordance with the frontier orbital. The frontier orbital gap helps to characterize the chemical reactivity, optical polarizability and chemical hardness–softness of a molecule. The small HOMO–LUMO energy gap means low excitation energy for the compound, a good stability and a low chemical hardness. The molecules having a large energy gap are known as hard, and molecules having a small energy gap are known as soft molecules. The soft molecules are more polarizable than the hard ones, because they need small energy for excitation. On the basis of Koopman's theorem, global reactivity descriptors are calculated using the energies of the frontier molecular orbitals E_{HOMO}, E_{LUMO} and given by Equations (1)–(5).

$$\chi = -(E_{HOMO} + E_{LUMO})/2 \quad (1)$$

$$\mu = -\chi = (E_{HOMO} + E_{LUMO})/2 \quad (2)$$

$$\eta = (-E_{HOMO} + E_{LUMO})/2 \quad (3)$$

where E_{HOMO} and E_{LUMO} are the energies of the HOMO and LUMO molecular orbitals. The value of η of BCNU, -1.131 eV, indicates for the compound should be a soft material. Softness (*S)* is the reciprocal of hardness and is a property of a compound that measures the extent of chemical reactivity.

$$S = 1/\eta \quad (4)$$

Parr *et al*. have proposed electrophilicity index (ω x) as a measure of energy lowering due to maximal electron flow between donor and acceptor. They defined electrophilicity index (ω) as follows

$$\omega = \mu 2\ S = \mu 2/\eta \quad (5)$$

The energies of frontier molecular orbitals (E_{HOMO}, E_{LUMO}), energy band gap (E_{HOMO}, E_{LUMO}), electro negativity (χ), the chemical potential (μ), hardness (η), softness (S) and electrophilicity index (ω) for BCNU are listed in Table 4.

Total, partial, and overlap population density-of-states

To provide a pictorial representation of MO compositions and their contributions to chemical bonding, The TDOS, PDOS and OPDOS density of states of the BCNU molecule are plotted in Figs. 8-10, respectively, created by convoluting the molecular orbital information with Gaussian curves of unit height and Full width at half maximum (FWHM) of 0.3 eV using the GaussSum 2.2 program. The DOS (or TDOS) plot is to the presentation of molecule orbital (MO) compositions and their contributions to chemical bonding through the OPDOS (or COOP) plot. The bonding, anti-bonding and non-bonding natures of the interaction of the two orbitals, atoms or groups explain the OPDOS (or COOP) diagrams. The value can be positive, negative or zero, the OPDOS it indicates a bonding interaction (because of the positive overlap population), an anti-bonding interaction (due to negative overlap population) and non-bonding interactions, respectively (Chen *et al.,* 1998). Additionally, the OPDOS diagrams allow us to the determination and comparison of the donor–acceptor properties of the ligands and ascertain the bonding, non-bonding. In the boundary region, neighboring orbitals may show quasi degenerate energy levels. In such cases,

consideration of only the HOMO and LUMO may not yield a realistic description of the frontier orbitals (Hoffmann, 1988; Hughbanks and Hoffmann, 1983; Małecki, 2010). If one sees these Figs. 8-10 can conclude HOMO and LUMO energy construction and groups energy distribution (C=O and NN=O) and also defined the bonding character of the title molecule according to TDOS, PDOS and OPDOS figures respectively. As also seen Fig. 7 HOMO orbitals are localized on the nitrosourea and CCl group their contributions about 83% and 17% respectively.

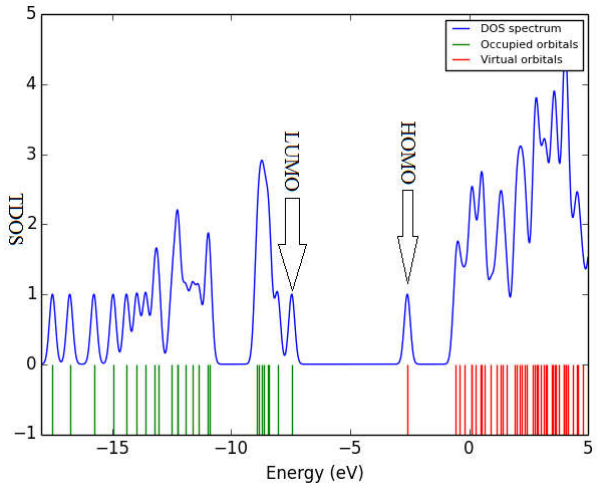

Fig. 8. The calculated TDOS diagrams for BCNU

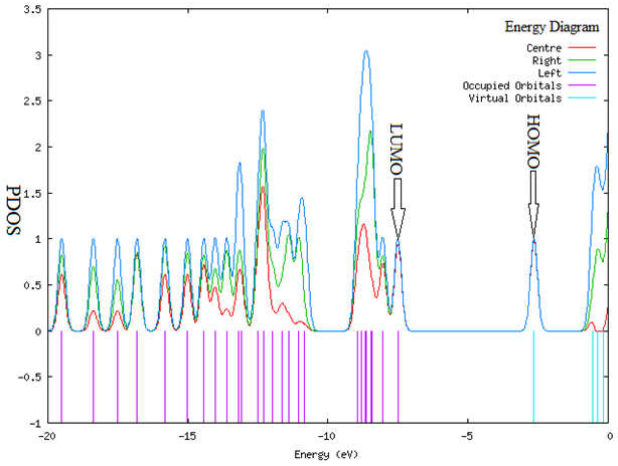

Fig. 9. The calculated PDOS diagrams for BCNU

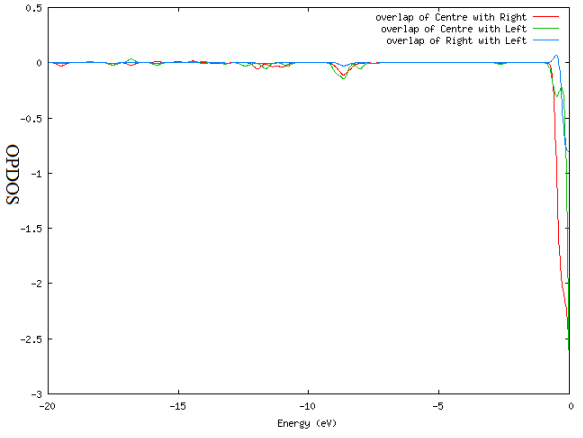

Fig. 10. The calculated OPDOS (or COOP) diagrams for BCNU

Similarly, the LUMO orbitals are localized on the nitrosourea (92%) and CCl groups (8%) of the compound. However, the OPDOS diagram is shown Fig. 10 and some of the orbitals of energy values of interaction between selected groups which are shown from figures easily, nitrosourea and CCl groups (blue line) system is negative (bonding interaction).

Thermodynamic function analysis

On the basis of the vibrational analysis and statistical thermodynamics, the standard thermodynamics functions; heat capacity at constant pressure (C_P), entropy (S) and enthalpy (H) are calculated using perl script THERMO.PL (Irikura and Thermo, 2002) and are listed in Table 5 and shown in figs. 11. As observed Table 6, the value of C_P, S and H, all increase of temperature from 100 to 1000 K there is an increment in all values, which is attributed to the enhancement of the molecular vibrations as the temperature increases (Bevan Ott and Boerio-Goates, 2000). The thermodynamic parameters supply helpful and extra information about the title molecule. Therefore, some values (such as the constant volume molar heat capacity (CV), entropy (S), zero-point vibrational energy (ZPVE), thermal energy correction (TE), total energies (E), and rotational constant) of the studied molecule by DFT/B3LYP/6-311++G(d,p) method at 298.15 K in ground state are listed in the Table 6.

Table 5. Thermodynamic properties at different temperatures at the B3LYP/6-311++ G(d,p) level for BCNU

Temperature (K)	C_p (J mol^{-1} K^{-1})	S (J mol^{-1} K^{-1})	H (kJ mol^{-1})
100.00	359.957	105.335	7.481
150.00	407.240	129.193	13.352
200.00	447.547	152.086	20.385
250.00	483.951	175.111	28.563
298.15	516.705	197.451	37.533
300.00	517.929	198.306	37.899
350.00	550.218	221.065	48.387
400.00	581.165	242.711	59.987
450.00	610.929	262.797	72.632
500.00	639.582	281.140	86.238
550.00	667.170	297.750	100.717
600.00	693.732	312.750	115.986
650.00	719.310	326.302	131.968
700.00	743.948	338.576	148.595
750.00	767.693	349.731	165.807
800.00	790.594	359.903	183.551
850.00	812.696	369.207	201.782
900.00	834.045	377.744	220.459
950.00	854.682	385.594	239.545
1000.00	874.647	392.828	259.008

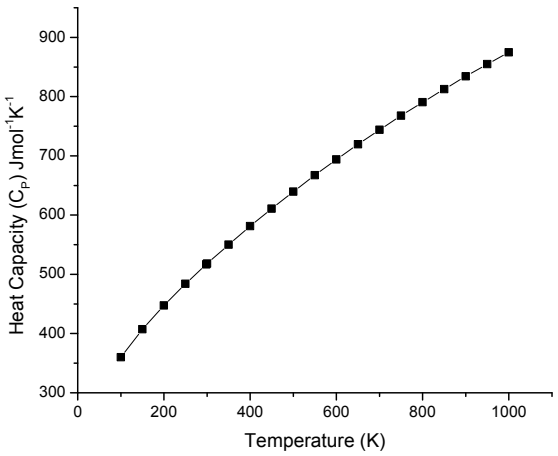

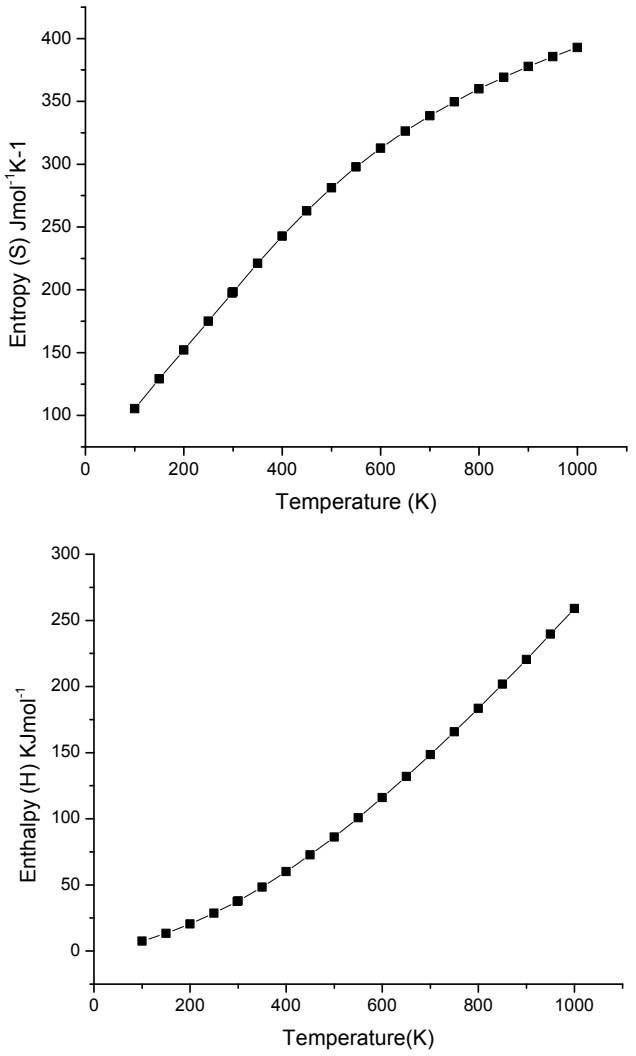

Fig. 11. The calculated heat capacity, entropy, enthalpy and temperature of BCNU

Table 6. Calculated Thermo-dynamical Properties[d] for the BCNU molecule

Parameters	BCNU
Total energy (E)	-1431.212
Zero point vibrational energy (ZPVE)	98.127
Contribution to the thermal energy correction (TE)	106.506
Constant volume molar heat capacity (CV)	45.205
Entropy (S)	123.469
Rotational Constant (RC)	
a 1.596	
b	0.253
c	0.230

[d] E are measured in Hartrees, ZPVE & TE are measured in Kcal/Mol, C_V & S are measured in Cal/Mol-Kelvin and Rotational Constant is measured in GHZ.

The global minimum energy obtained for structure optimization of the B3LYP with 6-311++G (d,p) basis set is -1431.212 Hartree (Table 6).

Hyperpolarizability analysis

In this study, the electronic dipole moment(μ), molecular polarizability(α), anisotropy of polarizability(Δα) and molecular first hyper polarizability(β) of BCNU are calculated using B3LYP/6-311++G** basis set, based on the finite-field approach. In the presence of an applied electric field, the energy of a system is a function of the electric field. First hyperpolarizability is a third rank tensor that can be described by a 3 × 3 × 3 matrix. The 27 components of the 3D matrix can be reduced to 10 components due to the Kleinman symmetry (Kleimman, 1962). It can be given in the lower tetrahedral format. It is obvious that the lower part of the 3 × 3 × 3 matrix is a tetrahedral. The components of ˇ are defined as the coefficients in the Taylor series expansion of the energy in the external electric field. When the external electric field is weak and homogeneous, this expansion becomes:

$$E = E^{\circ} - \mu_{\alpha}F_{\alpha} - \frac{1}{2}\alpha_{\alpha\beta}F_{\alpha}F_{\beta} - \frac{1}{6}\beta_{\alpha\beta\gamma}F_{\alpha}F_{\beta}F_{\gamma} \quad (1)$$

where E° is the energy of the unperturbed molecules, F_{α} the field at the origin μ_{α} , $\alpha_{\alpha\beta}$ *and* $\beta_{\alpha\beta\gamma}$ are the components of dipole moment, polarizability and the first hyperpolarizabilities, respectively. The total static dipole moment(μ), molecular polarizability(α), anisotropy of polarizability(Δα) and molecular first hyper polarizability(β) using the x, y, z components they are defined as

$$\mu = \sqrt{\left(\mu_x^2 + \mu_y^2 + \mu_z^2\right)} \quad (2)$$

$$\alpha = \left(\frac{\alpha_{xx}+\alpha_{yy}+\alpha_{zz}}{3}\right) \quad (3)$$

$$\Delta\alpha = \sqrt{\left[\left(\alpha_{xx} - \alpha_{yy}\right)^2 + \left(\alpha_{yy} - \alpha_{zz}\right)^2 + \left(\alpha_{zz} - \alpha_{xx}\right)^2 + 6\alpha_{xz}^2 + 6\alpha_{xy}^2 + 6\alpha_{yz}^2\right]} \quad (4)$$

$$\beta = \sqrt{\left[\left(\beta_{xxx} + \beta_{xyy} + \beta_{xzz}\right)^2 + \left(\beta_{yyy} + \beta_{xxy} + \beta_{yzz}\right)^2 + \left(\beta_{xxz} + \beta_{yyz} + \beta_{zzz}\right)^2\right]} \quad (5)$$

and

$$\beta_{total} = \sqrt{\left(\beta_{xxx}^2 + \beta_{yyy}^2 + \beta_{zzz}^2\right)} \quad (6)$$

In this study, the computation of dipole moment, molecular polarizability and hyper polarizability of BCNU is shown in Table 7. The value of the dipole moment μ, polarizabilities α and the hyperpolarizability β can be obtained by a frequency job output file of Gaussian 09 are reported in a atomic mass units (a.u.), the calculated values have been converted into electrostatic units (esu) (α: 1 a.u = 0.1482×10^{-24} esu; β: 1 a.u= 8.6393×10^{-33}esu). The B3LYP/6-311++G (d,p) results of electronic dipole moment μ_i (i = x, y, z), polarizability α_{ij} and first order hyperpolarizability β_{ijk} are listed in Table 7. The calculated dipole moment is equal to 12.339 Debye. The highest value of dipole moment is observed for the component μ_z while μ_x is the smallest one.

In this direction, these values are equal to 5.724 Debye (μ_z). For direction x and y, these values are equal to −9.236 Debye and -5.846 Debye, respectively. It is well known that the higher value of dipole moment, molecular polarizability and hyper polarizability are important for more active nonlinear optical (NLO) properties. The calculated mean polarizability α is equal to 5.552 a. u. The magnitude of the molecular hyperpolarizability (β) is one of the important key factors in a NLO system. As we can see in Table 7, the value of first hyperpolarizability (β) and total hyperpolarizability (β_{total}) for the title compound is equal to 11.241 and 5.302 a.u respectively.

Table 7. Calculated Electrical Properties[e] of the BCNU molecule

Parameters	BCNU
μ_x	-9.236
μ_y	-5.846
μ_z	5.724
Dipole moment (μ)	12.339
α_{xx}	1.471
α_{xy}	-2.690
α_{yy}	1.205
α_{xz}	-7.019
α_{yz}	1.423
α_{zz}	8.626
Mean Polarizability(α)	5.552
Polarizability anisotropy($\Delta\alpha$)	7.291
β_{xxx}	-1.337
β_{xxy}	-1.394
β_{xyy}	-7.621
β_{yyy}	5.005
β_{xxz}	-1.562
β_{xyz}	1.575
β_{yyz}	3.418
β_{xzz}	-1.726
β_{yzz}	-1.795
β_{zzz}	1.133
First hyperpolarizability(β)	11.241
Total hyperpolarizability (β_{total})	5.302

[e] μ is measured in Debye and α, $\Delta\alpha$, β and β_{total} are measured in a.u.

Electrostatic potential

Electrostatic potential (ESP) useful quantities to illustrate the charge distributions of molecules are used to visualize variably charged regions of a molecule. Therefore the charge distribution can give the information about how the molecules interact with another molecule. The value and spatial distribution of ESP are in fact responsible for the chemical behavior of an agent in a chemical reaction (Murray and Murray, 1996; Scrocco *et al.,* 1978). They strongly influence the binding of a substrate to its active site. ESP is typically visualized through mapping its values onto the molecular ED. The different values of the electrostatic potential at the surface are represented by different colors; red represents regions of most negative electrostatic potential, blue represents regions of most positive electrostatic potential and green represents regions of zero potential. Potential increases in the order red, orange, yellow, green and blue. While the negative electrostatic potential corresponds to an attraction of the proton by the concentrated ED in the molecule (and is colored in shades of red), the positive electrostatic potential corresponds to the repulsion of the proton by atomic nuclei in regions where low ED exists and the nuclear charge is incompletely shielded (and is colored in shades of blue). The total and alpha densities plot for BCNU molecule are shown in Fig. 12 and their arrays are reproduced in Fig. 13. The ESP of the titled molecule and its array are shown in Figs. 14 and 15 respectively. These figures provide a visual representation of the chemically active sites and comparative reactivity of atoms.

Natural bond orbital analysis

The natural bond orbital (NBO) calculations were performed on BCNU using NBO 3.1 program (Glendening *et al.,* 1996) as implemented in the Gaussian09 package at the DFT/B3LYP level of theory in order to elucidate intermolecular hydrogen bonding and intermolecular charge transfer (ICT) interactions.

The second order Fock matrix (perturbation theory analysis) was carried out to determine the donor–acceptor interactions in NBO basis of the molecule. The results of interactions showed that in a loss of occupancy from the localized.NBO of the idealized Lewis structure into an empty non-Lewis orbital. For each donor (i) and acceptor (j), the stabilization energy $E^{(2)}$ associated with the delocalization i → j is estimated as

$$E^{(2)} = \Delta E_{i,j} = q_j \frac{F(i,j)^2}{\epsilon_i - \epsilon_j} \quad (1)$$

Where q_i is the donor orbital occupancy, ε_i and ε_j are diagonal elements and F (i,j) is the off diagonal NBO Fock matrix element.

An efficient method is NBO analysis for studying intra- and inter-molecular bonding, interaction among bonds and investigating charge transfer or conjugative interaction in molecular systems. The most accurate possible "natural Lewis structure" picture of φ is supplied NBO analysis, using the highest possible percentage of the electron density for all orbital details chosen mathematically. This analysis gives information about interactions in both occupied and unoccupied orbital spaces that could enhance the analysis of intra- and inter-molecular interactions.

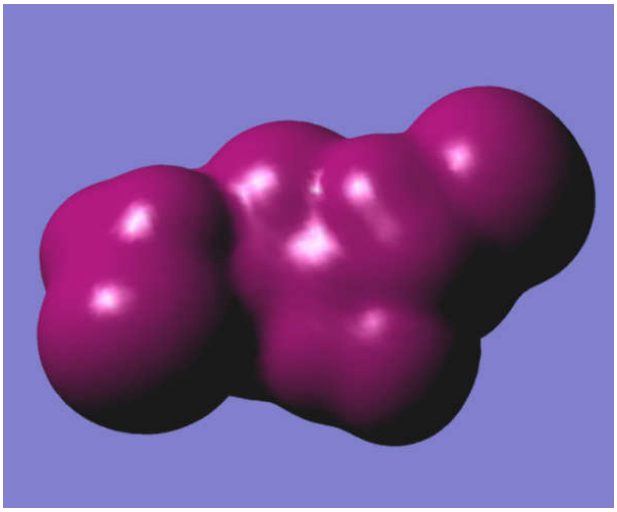

(a)

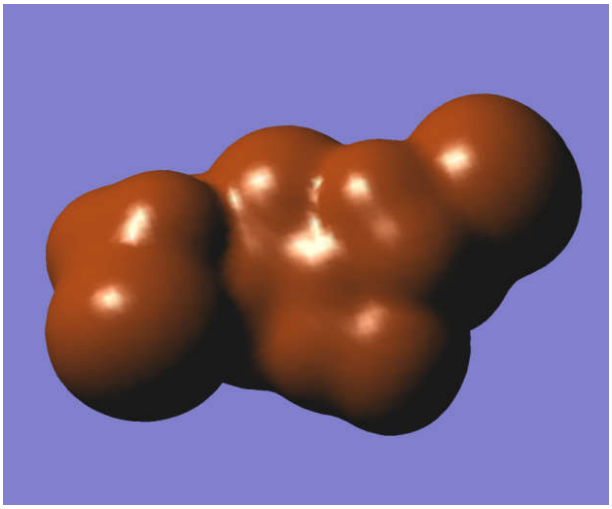

(b)

Fig. 12. (a) Total (b) alpha SCF densities of BCNU

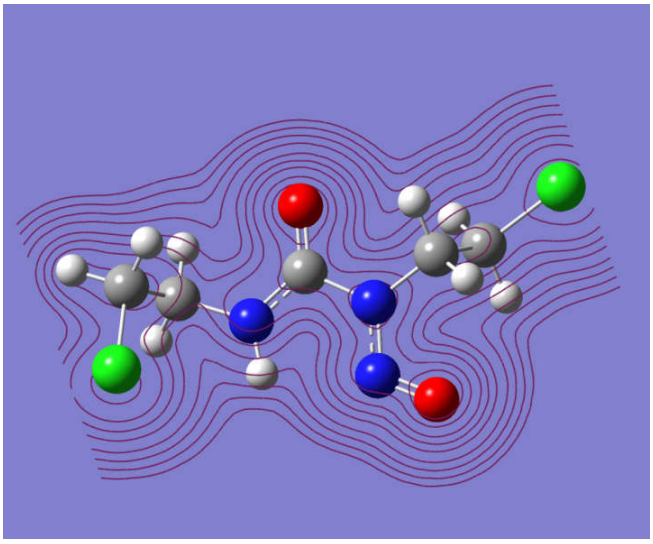

(a)

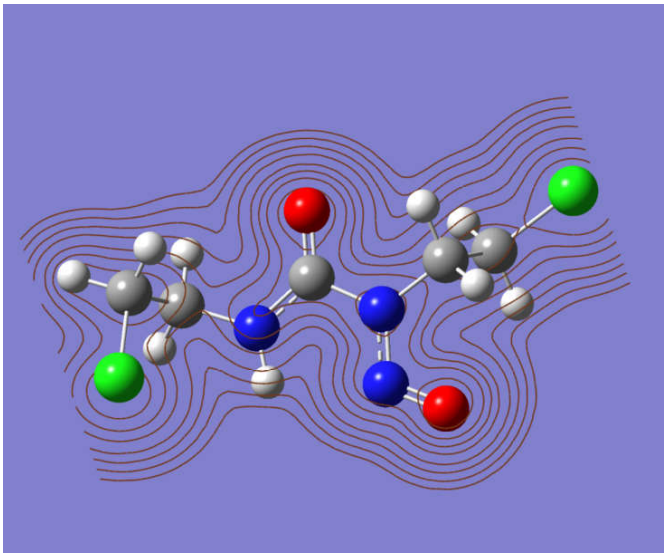

(b)

Fig. 13. (a) Total (b) alpha SCF density arrays of BCNU

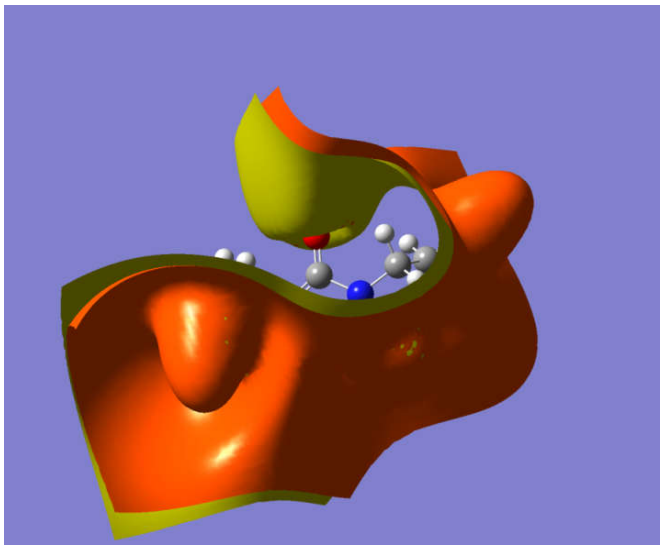

Fig. 14. Electrostatic potential of BCNU

The interacting stabilization energy resulting from the second-order micro-disturbance theory and some electron donor orbital, acceptor orbital are published. Table 8 depicts the bonding concepts such as type of bond orbital, their occupancies, the natural atomic hybrids of which the NBO is composed, giving the percentage of the NBO on each hybrid, the atom label, and a hybrid label showing the hybrid orbital (sp^x) composition (the amount of s-character, p character, etc.) of BCNU molecule. From Table 8, it is clear that the BD (1) N1-N6 orbital having 1.99142 has 54.29% N1 character in a $sp^{2.33}$ hybrid and 45.71% N6 character in a $sp^{3.10}$ hybrid. The $sp^{2.33}$ hybrid on N has 69.93% p-character and the $sp^{3.10}$ hybrid on N has 75.47% p-character.

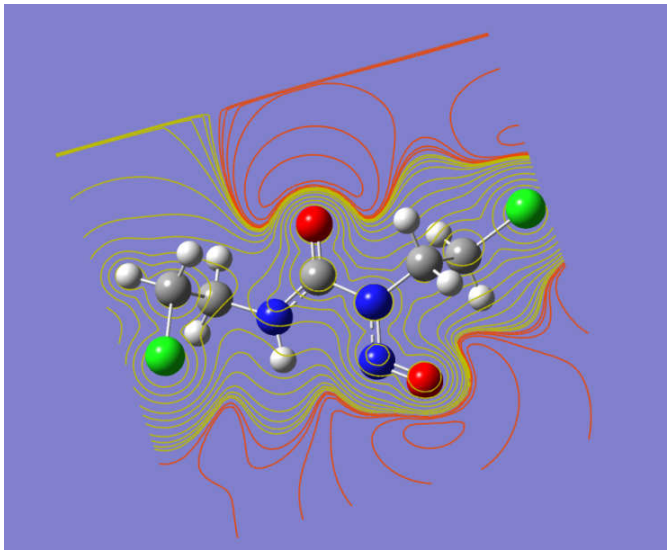

Fig. 15. Electrostatic potential array of BCNU

The BD (1) C2-O5 orbital having 1.99175 has 35.97% N1 character in a $sp^{1.86}$ hybrid and 64.03% O5 character in a $sp^{1.51}$ hybrid. The $sp^{1.86}$ hybrid on C has 64.91% p-character and the $sp^{1.51}$ hybrid on O has 60.07% p-character. An idealized sp^3 hybrid has 75% p-character. The lone pair (LP) which are expected to the attain Lewis structure are given at the end of Table 8. The variations in energies are shown in Table 8 and these variations in energies are because of inter- and intra-molecular interactions of the molecules. The larger $E^{(2)}$ (energy of hyper conjugative interactions) value shows the intensive interaction between electron-donors and electron-acceptors i.e. the more donating tendency from electron donors to electron acceptors, and greater the extent of conjugation of the whole system, so the possible intensive interactions are given in Table 9. The second-order perturbation theory analysis of Fock matrix in NBO basis shows strong intra-molecular hyperconjugative interactions of electrons. The intra-molecular interactions are formed by the orbital overlap between $\sigma \rightarrow \sigma^*$, $LP \rightarrow \sigma^*$, $LP \rightarrow RY^*(1)$,$\sigma \rightarrow RY^*(1)$ bond and orbital which results intra-molecular charge transfer (ICT) causing stabilization of the system (Table 9). These interactions are observed as increase in electron density (ED) in C-C anti-bonding orbital that weakens the respective bonds. The electron density of conjugated bond of aromatic ring (ca. 1.99e) clearly demonstrates strong delocalization. The interaction between lone pair (LP) N3, O5, N6, O7 and O14 with antibonding orbital of $\sigma*$ and $RY*(1)$ are presented in Table 9. The LP N3 and N6 lead to delocalized to the antibonding σ^*(C15-C17) and σ^*(N1-C8) with stabilization energy 6.78 and 9.74 kJ/mol, respectively. Further LP(1)O5 leads to strong delocalized to the antibonding RY*(1)C2 with stabilization energy 16.99kJ/mol.

Table 8. NBO analysis of BCNU molecule based on B3LYP/6-311++G(d,p) method

Bond(A-B)	ED/ Energy	ED_A %	ED_B %	NBO	S %	P %
BD(1) N1-C2	1.98354	63.68%	36.32%	$0.7980sp^{1.95}$	33.93%	66.03%
				$0.6026sp^{2.39}$	29.43%	70.45%
BD(1) N1-N6	1.99142	54.29%	45.71%	$0.7368sp^{2.33}$	29.98%	69.93%
				$0.6761sp^{3.10}$	24.37%	75.47%
BD(1) N1-C8	1.98558	63.96%	36.04%	$0.7997sp^{1.77}$	36.07%	63.91%
				$0.6003sp^{3.74}$	21.08%	78.77%
BD(1) C2-N3	1.98792	38.75%	61.25%	$0.6225sp^{1.81}$	35.52%	64.38%
				$0.7826\ sp^{1.81}$	35.57%	64.37%
BD(1) C2-O5	1.99175	35.97%	64.03%	$0.5998sp^{1.86}$	34.94%	64.91%
				$0.8002sp^{1.51}$	39.80%	60.07%
BD(1) N3-H4	1.98269	71.95%	28.05%	$0.8482sp^{2.43}$	29.14%	70.82%
				$0.5297sp^{0.00}$	99.93%	0.07%
BD(1) N3-C15	1.98703	62.50%	37.50%	$0.7906sp^{1.85}$	35.12%	64.86%
				$0.6124sp^{3.41}$	22.64%	77.22%
BD(1) N6-O7	1.99325	37.96%	62.04%	$0.6161sp^{99.99}$	0.55%	99.03%
				$0.7876sp^{99.99}$	0.47%	99.36%
BD(1) C8-H9	1.97722	61.94%	38.06%	$0.7870sp^{3.05}$	24.69%	75.24%
				$0.6170sp^{0.00}$	99.96%	0.04%
BD(1) C8-H10	1.97748	62.24%	37.76%	0.7889sp2.99	25.07%	74.86%
				0.6145sp0.00	99.96%	0.04%
BD(1) C8-C11	1.98364	50.02%	49.98%	0.7072sp2.41	29.28%	70.67%
				0.7070sp2.27	30.57%	69.38%
BD(1) C11-H12	1.98809	61.07%	38.93%	0.7815sp2.92	25.49%	74.44%
				0.6239sp0.00	99.96%	0.04%
BD(1) C11-H13	1.98759	61.06%	38.94%	0.7814sp2.93	25.45%	74.48%
				0.6241sp0.00	99.96%	0.04%
BD(1) C11-Cl14	1.98754	44.44%	55.56%	0.6666sp4.38	18.55%	81.27%
				0.7454sp5.77	14.71%	84.78%
BD(1) C15-H16	1.98148	60.53%	39.47%	0.7780sp3.26	23.47%	76.46%
				0.6283sp0.00	99.96%	0.04%
BD(1) C15-C17	1.98924	49.74%	50.26%	0.7052sp2.37	29.63%	70.32%
				0.7090sp2.25	30.72%	69.24%
BD(1) C15-H20	1.97119	61.61%	38.39%	0.7849sp3.09	24.46%	75.48%
				0.6196sp0.00	99.96%	0.04%
BD(1) C17-H18	1.98435	60.87%	39.13%	0.7802sp3.01	24.91%	75.02%
				0.6256sp0.00	99.96%	0.04%
BD(1) C17-H19	1.98694	61.16%	38.84%	0.7820sp2.95	25.32%	74.61%
				0.6232sp0.00	99.96%	0.04%
BD(1) C17-Cl21	1.99063	44.11%	55.89%	0.6642sp4.21	19.16%	80.66%
				0.7476sp5.82	14.58%	84.91%
LP(1) N1	1.57778	-	-	sp 1.00	0.01%	99.97%
LP(1) N3	1.70596	-	-	sp99.99	0.12%	99.86%
LP(1) O5	1.97888	-	-	sp 0.66	60.21%	39.77%
LP(1) N6	1.95370	-	-	sp 1.09	47.80%	52.16%
LP(1) O7	1.98865	-	-	sp 0.38	72.25%	27.74%
LP(1)Cl14	1.99724	-	-	sp 0.18	84.76%	15.23%
LP(1)Cl21	1.99717	-	-	sp 0.17	85.24%	14.75%
BD*(1) N1-C2	0.10224	36.04%	63.96%	0.6003sp1.77	33.93%	66.03%
				-0.7997sp3.74	29.43%	70.45%
BD*(1) N1-N6	0.08366	36.32%	63.68%	0.6026sp1.95	29.98%	69.93%
				-0.7980sp2.39	24.37%	75.47%
BD*(1) N1-C8	0.04792	45.71%	54.29%	0.6761sp2.33	36.07%	63.91%
				-0.7368sp3.10	21.08%	78.77%
BD*(1) C2-N3	0.06507	61.25%	38.75%	0.7826sp1.81	35.52%	64.38%
				-0.6225sp1.81	35.57%	64.37%
BD*(1) C2-O5	0.01173	64.03%	35.97%	0.8002sp1.86	34.94%	64.91%
				-0.5998sp1.51	39.80%	60.07%
BD*(1) N3-H4	0.02325	28.05%	71.95%	0.5297sp2.43	29.14%	70.82%
				-0.8482sp0.00	99.93%	0.07%
BD*(1) N3-C15	0.02109	37.50%	62.50%	0.6124sp1.85	35.12%	64.86%
				-0.7906sp3.41	22.64%	77.22%
BD*(1) N6-O7	0.31582	62.04%	37.96%	0.7876sp99.99	0.55%	99.03%
				0.6161sp99.99	0.47%	99.36%
BD*(1) C8-H9	0.01725	38.06%	61.94%	0.6170sp3.05	24.69%	75.24%
				-0.7870sp0.00	99.96%	0.04%
BD*(1) C8-H10	0.01394	37.76%	62.24%	0.6145sp2.99	25.07%	74.86%
				-0.7889sp0.00	99.96%	0.04%
BD*(1) C8-C11	0.02248	49.98%	50.02%	0.7070sp2.41	29.28%	70.67%
				-0.7072sp2.27	30.57%	69.38%
BD*(1)C11-H12	0.01878	38.93%	61.07%	0.6239sp2.92	25.49%	74.44%
				-0.7815sp0.00	99.96%	0.04%
BD*(1) C11-H13	0.01886	38.94%	61.06%	0.6241sp2.93	25.45%	74.48%
				-0.7814sp0.00	99.96%	0.04%
BD*(1) C11-Cl14	0.01634	55.56%	44.44%	0.7454sp4.38	18.55%	81.27%
				-0.6666sp5.77	14.71%	84.78%

Continue……

BD*(1) C15-H16	0.01569	39.47%	60.53%	0.6283sp3.26	23.47%	76.46%
				-0.7780sp0.00	99.96%	0.04%
BD*(1) C15-C17	0.02858	50.26%	49.74%	0.7090sp2.37	29.63%	70.32%
				-0.7052sp2.25	30.72%	69.24%
BD*(1) C15-H20	0.01519	38.39%	61.61%	0.6196sp3.09	24.46%	75.48%
				-0.7849sp0.00	99.96%	0.04%
BD*(1) C17-H18	0.01811	39.13%	60.87%	0.6256sp3.01	24.91%	75.02%
				-0.7802sp0.00	99.96%	0.04%
BD*(1) C17-H19	0.02020	38.84%	61.16%	0.6232sp2.95	25.32%	74.61%
				-0.7820sp0.00	99.96%	0.04%
BD*(1) C7-Cl21	0.02127	55.89%	44.11%	0.7476sp4.21	19.16%	80.66%
				-0.6642sp5.82	14.58%	84.91%

Table 9. Second order Perturbation theory analysis of Fock matrix in NBO basis for BCNU

Donor (i)	Type	E_D (i) (e)	Acceptor (j)	Type	E_D (j) (e)	E(2)[a] kcal/mol	E(j)-E(i)[b] a.u.	$F(i,j)$[c] a.u.
N1-C2	σ	1.98354	C8	RY*(1)	0.00827	1.41	1.54	0.042
			N3-C15	σ*	0.02109	2.75	1.13	0.050
N1-N6	σ	1.99142	C2	RY*(1)	0.01717	0.65	2.04	0.033
			O7	RY*(1)	0.00445	1.01	1.88	0.039
			C8	RY*(1)	0.00827	0.59	1.65	0.028
			N1-C8	σ*	0.04792	0.69	1.22	0.026
			C2-O5	σ*	0.01173	1.33	1.50	0.040
N1-C8	σ	1.98558	C2	RY*(1)	0.01717	1.33	1.90	0.045
			N6	RY*(1)	0.01056	0.61	2.10	0.032
			N1-C2	σ*	0.10224	0.61	1.10	0.024
			C2-N3	σ*	0.06507	1.56	1.24	0.040
			C11-Cl14	σ*	0.01634	2.07	0.88	0.038
C2-N3	σ	1.98792	N1	RY*(1)	0.01166	0.51	1.56	0.025
			C15	RY*(1)	0.00623	1.36	1.59	0.042
			N1-C8	σ*	0.04792	2.06	1.17	0.044
			C2-O5	σ*	0.01173	2.03	1.45	0.048
			N3-H4	σ*	0.02325	0.66	1.27	0.026
			N3-C15	σ*	0.02109	0.77	1.19	0.027
C2-O5	σ	1.99175	C2	RY*(1)	0.01717	1.50	2.21	0.052
			N1-C2	σ*	0.10224	0.53	1.41	0.025
			N1-N6	σ*	0.08366	1.46	1.43	0.042
			C2-N3	σ*	0.06507	2.14	1.55	0.052
			N3-H4	σ*	0.02325	1.20	1.49	0.038
N3-H4	σ	1.98269	C15	RY*(1)	0.00623	0.74	1.40	0.029
			N1-C2	σ*	0.10224	0.95	1.00	0.028
			C2-O5	σ*	0.01173	5.42	1.26	0.074
			C15-H20	σ*	0.01519	0.96	1.07	0.029
N3-C15	σ	1.98703	C2	RY*(1)	0.01717	1.67	1.89	0.050
			N1-C2	σ*	0.10224	3.05	1.08	0.052
			C2-N3	σ*	0.06507	1.20	1.22	0.035
			C17-H18	σ*	0.01811	0.86	1.14	0.028
N6-O7	σ	1.99325	N6-O7	σ*	0.31582	1.77	0.38	0.025
C8-H9	σ	1.97722	N1-C2	σ*	0.10224	3.17	0.85	0.047
			C11-H13	σ*	0.01886	2.23	0.92	0.040
C8-H10	σ	1.97748	N1-N6	σ*	0.08366	4.27	0.87	0.055
			C11-H12	σ*	0.01878	2.29	0.92	0.041
C8-C11	σ	1.98364	Cl14	RY*(1)	0.00210	0.71	1.30	0.027
			N1-C2	σ*	0.10224	0.70	0.97	0.024
			C8-H9	σ*	0.01725	0.51	1.05	0.021
			C8-H10	σ*	0.01394	0.51	1.06	0.021
C11-H12	σ	1.98809	C8	RY*(1)	0.00827	0.92	1.27	0.030
			C8-H10	σ*	0.01394	2.21	0.94	0.041
			C11-Cl14	σ*	0.01634	0.87	0.64	0.021
C11-H13	σ	1.98759	C8-H9	σ*	0.01725	2.33	0.93	0.042
			C11-Cl14	σ*	0.01634	0.87	0.64	0.021
C11-Cl14	σ	1.98754	N1-C8	σ*	0.04792	2.78	0.95	0.046
C15-H16	σ	1.98148	C2-N3	σ*	0.06507	2.94	0.99	0.049
			C17-H19	σ*	0.02020	2.39	0.91	0.042
C15-C17	σ	1.98924	N3	RY*(1)	0.00655	1.89	1.31	0.045
			Cl21	RY*(1)	0.00232	0.59	1.27	0.024
			C2-N3	σ*	0.06507	0.58	1.12	0.023
C15-H20	σ	1.97119	N3-H4	σ*	0.02325	3.34	0.93	0.050
			C17-Cl21	σ*	0.02127	5.01	0.62	0.050
C17-H18	σ	1.98435	N3-C15	σ*	0.02109	3.84	0.86	0.051
			C17-Cl21	σ*	0.02127	1.03	0.63	0.023
C17-H19	σ	1.98694	C15	RY*(1)	0.00623	0.85	1.26	0.029
			C15-H16	σ*	0.01569	2.45	0.92	0.042
			C17-Cl21	σ*	0.02127	1.07	0.63	0.023

Continue……

C17-Cl21	σ	1.99063	C15	RY*(1)	0.00623	0.53	1.37	0.024
			C15-H20	σ*	0.01519	1.64	1.04	0.037
N1	LP(1)	1.57778	N6-O7	σ*	0.31582	65.93	0.21	0.109
			C8-H9	σ*	0.01725	1.60	0.69	0.033
			C8-H10	σ*	0.01394	1.11	0.70	0.028
			C8-C11	σ*	0.02248	5.47	0.65	0.059
			C11-Cl14	σ*	0.01634	1.42	0.40	0.024
N3	LP(1)	1.70596	C15-H16	σ*	0.01569	2.04	0.65	0.035
			C15-C17	σ*	0.02858	6.78	0.62	0.062
			C15-H20	σ*	0.01519	1.26	0.66	0.028
			C17-H18	σ*	0.01811	0.75	0.65	0.021
O5	LP(1)	1.97888	C2	RY*(1)	0.01717	16.99	1.83	0.158
			N1-C2	σ*	0.10224	1.06	1.03	0.030
			C2-N3	σ*	0.06507	1.93	1.17	0.043
N6	LP(1)	1.95370	N1	RY*(1)	0.01166	2.20	1.19	0.046
			O7	RY*(1)	0.00445	1.38	1.47	0.041
			N1-C8	σ*	0.04792	9.74	0.80	0.079
			N3-H4	σ*	0.02325	2.04	0.90	0.038
O7	LP(1)	1.98865	N1-N6	σ*	0.08366	0.57	1.14	0.023
			N1-C8	σ*	0.04792	0.65	1.10	0.024
Cl4	LP(1)	1.99724	C11	RY*(1)	0.00323	0.55	1.80	0.028
N1-C2	σ	1.99717	N1-N6	σ*	0.08366	5.43	0.02	0.034
			N3-H4	σ*	0.02325	2.30	0.08	0.049
			C8-H9	σ*	0.01725	0.78	0.08	0.029
			C8-H10	σ*	0.01394	1.12	0.09	0.037

E_D means Electron Density.
[a]E(2) means energy of hyper conjugative interactions.
[b]Energy difference between donor and acceptor iand j NBO orbitals.
[c]F(I,j) is the Fock matrix element between I and j NBO orbitals.

Reduced density gradient (RDG)

In order to investigate the weak interactions in real space based on the electron density and its derivatives were developed an approach (Johnson *et al.,* 2010). The RDG is a fundamental dimensionless quantity coming from the density and its first derivative:

$$RDG(r) = \frac{1}{2\sqrt[3]{(3\pi^2)}} \frac{|\nabla\rho(r)|}{\rho(r)^{4/3}} \quad \ldots\ldots\ldots\ldots\ldots\ldots\ldots\ldots (1)$$

The weak interactions are shown in the region with low electron density and low RDG. The electron density ρ (plot of the RDG versus) multiplied by the sign of λ_2 can permit investigation and visualization of a wide range of interactions types. RDG density tails show that; large, negative values of sign $(\lambda_2)\rho$ are indicative of attractive interactions (such as dipole–dipole or hydrogen bonding); while if sign$(\lambda_2)\rho$ is large and positive, the interaction is non-bonding. Values near zero indicate very weak, van der Waals interactions. The sign of λ_2 is utilized to distinguish the bonded ($\lambda_2 < 0$) from non-bonded ($\lambda_2 > 0$) interactions (34). The RDG of BCNU were graphed by Multiwfn and plotted by VMD program (Rozas *et al.,* 2000; Bader, 1990) respectively, and this representation is given in Fig.16. According to this representation of the RDG showed non-bonded ($\lambda_2 > 0$) interactions and red indicates strong non-bonded overlap. The RDG of the molecule is plotted in Fig. 17. The RDG versus sign $(\lambda_2)\rho$ peaks (electron density value) itself provides the information about the strength of interaction. The RDG = 0.2 lines are evaluated in this molecule and crossed not only the attractive but also the repulsion spikes. Large, negative values of sign $(\lambda_2)\rho$ are indicative of stronger attractive interactions (spikes in the left part in Fig. 17), while positive ones, strong repulsion interactions (spikes in the right part in Fig. 17). Values near zero indicated very weak Van der Waals interactions. The weak interaction region can be located by generating RDG isosurface enclosing the corresponding regions in the real molecular space (Fig. 16). The gradient isosurfaces are colored to the values of sign $(\lambda_2)\rho$, which is found to be a good indicator of interaction strength shown in Fig. 17. The color from blue to red means from stronger attraction to repulsion, respectively. The center of ring of the title molecule showed that strong steric effect, filled by red color. The green color can be identified as Van der Waals (VDW) interaction region, which means that density electron in these regions are low. The RDG of the molecule is contributed in the literature.

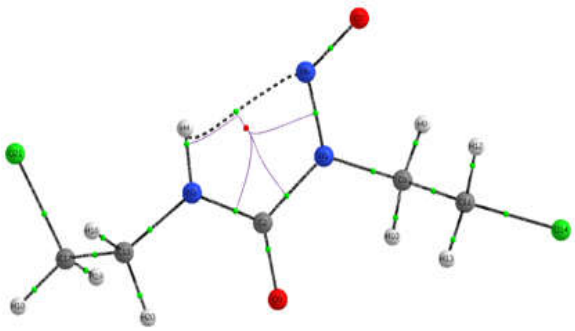

Fig. 16. H-Bond Interaction of BCNU

Atom in molecule (AIM) calculation

The topological analysis of atoms in the molecule provides us more effective information about the presence of strong and weak hydrogen bonds in terms of electron density (ρ_{BCP}), Laplacian of electron density ($\nabla^2\rho_{BCP}$) at Bond critical points (rBCPs). As Rozas *et al.* (36) explained; hydrogen bond interactions can be classified as follows:

(i) Weak hydrogen bonds of electrostatic character $\nabla^2\rho(rBCP) > 0$ and $g(rBCP) + v(rBCP) > 0$.

(ii) Medium hydrogen bond of partially covalent nature $\nabla^2\rho(rBCP) > 0$ and $g(rBCP) + v(rBCP) < 0$.

(iii) Strong hydrogen bond of covalent nature $\nabla^2\rho(rBCP) < 0$ and $g(rBCP) + v(rBCP) < 0$.

where g(rBCP) + v(rBCP) is also known as total electron energy density, h(rBCP). The nature of IHB (Intermolecular hydrogen bond) can be determined using ratio of −g(rBCP)/v(rBCP). The value of −g(rBCP)/ v(rBCP) > 1 for IHB having non-covalent nature, and 0.5 < −g(rBCP)/ v(rBCP) < 1 for IHB having partly covalent nature. Prediction of IHB energy is one of the most important subjects in recent studies not only for its characterization, but also due to the role, it plays in numerous processes, for example, in hydration.

Molecular graph of BCNU using AIM program at B3LYP/6-311G++ (d,p) level is given in Fig. 16. Geometrical as well as topological parameter for bonds of interacting atoms of ENU is given in Table 10. AIM calculation suggests that hydrogen bond H4....N6 in BCNU is electrostatic in nature. Several theoretical theory (Bader, 1990; Prabaharan *et al.,* 2015) have been proposed to estimate hydrogen bond energy. One of the most useful of these methods has been explained by Espinosa *et al.* (Espinosa *et al*., 1998) who found that IHB energy may be correlated with the potential electron energy density at critical point by the expression: $E_{IHB} = 1/2v(rBCP)$. The calculated hydrogen bond energy (E_{HB}) of BCNU is - 4.455 Kcal/mol.

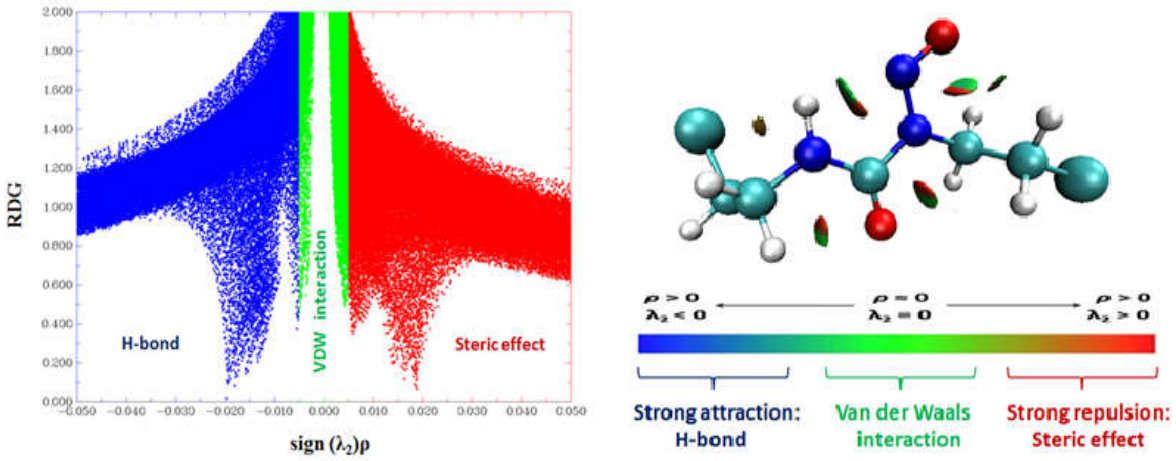

Fig. 17. Reduced density gradient for BCNU

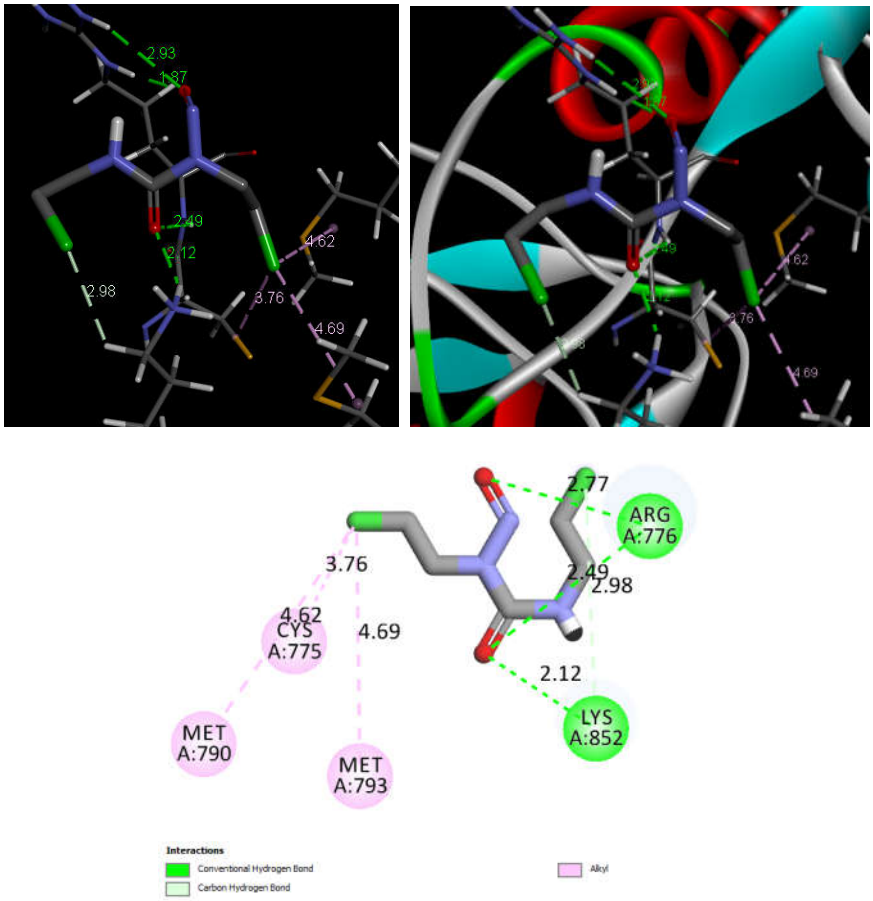

Fig. 18. Molecular docking interaction of the BCNU with 2JIU

Table 10. Geometrical parameter (bond length) and topological parameters for bonds of interacting atoms of BCNU : electron density(ρ_{BCP}), Laplacian of electron density($\nabla^2\rho_{BCP}$), electron kinetic energy density(G_{BCP}), electron potential energy density(V_{BCP}), total electron energy density(H_{BCP}), ellipticity(ε_{BCP}), hydrogen bond energy(E_{HB}) at bond critical point (BCP)

Interactions X-H....Y	Bond length H....Y (Å)	ρ_{BCP} (a.u)	$\nabla^2\rho_{BCP}$ (a.u)	G_{BCP} (a.u)	V_{BCP} (a.u)	H_{BCP} (a.u)	ε_{BCP} (a.u)	E_{IHB} (Kcal/mol)
N3-H4....N6	2.2075	0.0196	0.0855	0.0178	-0.0142	0.0036	0.4956	-4.4554

Table 11. Binding energy and hydrogen bond distance parameters for BCNU on binding with 2JIU protein

PDB ID	Nature of Bond	Bonded residues	Bond distance (Å)	Estimated inhibition constant (μm)	Binding energy (kcal/mol)
2JIU	Conventional H-Bond	ARG 776	2.77	721.28	-4.29
		ARG 776	2.49		
		LYS 852	2.12		
	Carbon H-Bond	LYS 852	2.98		
	Hydrophobic	CYS 775	3.76		
		MET 790	4.62		
		MET 793	4.69		

Molecular Docking analysis

The molecular docking is a computational procedure that attempts to predict the non-covalent binding of macromolecule (receptor) and a small molecule (ligands). Automated docking is widely used for the prediction of bimolecular complexes in structure/function analysis and in molecular design. Docking of small molecule compounds into the binding site of a receptor and estimating the binding affinity of the complex is an important part of the structure based drug design process (Ligand docking and binding site analysis with PyMOL, Autodock/Vina, Daniel Seeliger Bert L. de Groot, 2010). AutoDock Tools offers a complete molecular viewer and a graphical support for all steps required for setup and analysis of docking runs. To evaluate the anticancer activity of BCNU molecular docking studies were carried out against 2JIU protein. Molecular docking calculation was performed on AutoDock. The crystal structure of 2JIU is downloaded from RSCB PDB website. The AutoDock Tools graphical user interface was used to add polar hydrogen. Protein was cleaned by removing waters and co-crystallized ligand. The active site of enzyme was defined to include residues of the active site within the grid size of 60 Å x 60 Å x 60 Å. The most popular algorithm Lamarckian Genetic Algorithm (LGA) present in AutoDock was employed for docking. Among all docked conformations, the one which bound perfectly at the active site was examined through Discovery studio visualizer4.5 software (Discovery Studio 4.5 Guide, Accelrys Inc., San Diego, 2009) for the detailed interactions. Protein-ligand interaction between 2JIU and BCNU shows H-bond interaction with the amino acid (ARG 776, ARG 776 and LYS 852) having binding energy -4.29 kcal/mol as shown in Table 11 and Fig. 18.

Conclusion

The detailed interpretations of the molecular structure, vibrational spectra, electronic and Mulliken charge analysis; thermo-dynamical parameters and RDG as well as molecular docking of BCNU were presented in this paper. The geometrical parameters of BCNU were computed by DFT calculations as well as the correlations of the statistical thermodynamics according to temperature are also presented. All results which were examined before by the experimental (FT-IR, FT-Raman and UV spectra) were supported by the computed results, comparing with experimental characterization data; vibrational wavenumbers values are in fairly good agreement with the experimental results. The predicted calculations are compared with experimental and showed an acceptable general agreement. It is worth mentioning that, for our molecule, the stretching vibrational modes are CO, NN, CN, CH, CC, CCl, NO and NH. However, there is great mixing of the CH_2 vibrational modes. The descriptions of the modes are very complex because of the low symmetry of the studied molecule. Especially, in plane modes and out of plane modes are the most difficult to assigned due to mixing with the ring modes and also with the substituent modes. The most important energy gap (E_{HOMO}-E_{LUMO}, E_{HOMO}-E_{LUMO+1}, E_{HOMO-1}-E_{LUMO}) were calculated at 4.859, 5.458 and 6.892 eV for the BCNU molecule. The LP N3 and N6 lead to delocalized to the antibonding σ^*(C15-C17) and σ^*(N1-C8) with stabilization energy 6.78 and 9.74 kJ/mol, respectively. The gradient isosurfaces are colored to the values of sign(λ_2)ρ, which is found to be a good indicator of interaction strength. The color from blue to red means from stronger attraction to repulsion, respectively. The center of ring of the title molecule showed that strong steric effect, filled by red color. The green color can be identified as Van der Waals (VDW) interaction region, which means that density electron in these regions are low. The predicted first hyperpolarizability and molecular docking results on BCNU leaves the legacy and open up the way to extend its application in the field of non-linear optics and molecular drug designing.

Acknowledgements

This work was supported by the Department of Science and Technology (DST), New Delhi funded through research Grant No: SR/WOS-A/PM-1008/2015(G).

REFERENCES

Bader, R. F. W. 1990. "Atoms in Molecules A Quantum Theory, Oxford University Press, Oxford, U.K." Becke, A.D. 1993. "Density-functional thermochemistry. III. The role of exact exchange." J. Chem. Phys. 98 ;5648–5652.

Bevan Ott, J. and Boerio-Goates, J. 2000. "Calculations from Statistical Thermodynamics, Academic Press, *2000."*

Chattaraj, P.K., Maiti, B. and Sarkar, U. 2003. "Philicity: A Unified Treatment of Chemical Reactivity and Selectivity *"J. Phys. Chem.* A. 107(25); 4973-4975.

Chen, M., Waghmare, U.V., Friend, C.M. and Kaxiras, E. 1998. "A density functional study of clean and hydrogen-

covered α-MoO3 (010):α-MoO3(010): Electronic structure and surface relaxation"J. Chem. Phys., 109; 680–6854.

Choi, C.H. and Kertesz, M. 1997. "Conformational Information from Vibrational Spectra of Styrene, trans-Stilbene, and cis-Stilbene" *J. Phys. Chem*. 101(20); 3823-3831.

Dalili Mansour, N., Mahboubi, F. and Nahrjou, N. 2015." DFT/NBO analysis of interaction between a CNT and anti-cancer drugs" *Int. J. Nano Dimens*., 6(5);479-486.

Daniel Seeliger Bert L. de Groot,. (2010. "Ligand docking and binding site analysis with PyMOL, Autodock/Vina." J. Comput. Aided Mol. Des. 24; 417–422.

Discovery Studio 4.5 Guide, Accelrys Inc., San Diego, http://www.accelrys.com, 2009.

Espinosa, E., Molins, E. and Lecomte, C. 1998. "Hydrogen bond strengths revealed by topological analyses of experimentally observed electron densities"Chem. Phys. Lett., 285(3);170-173.

Ewend M. G., Brem S., and Gilbert M. 2007. "Treatment of single brain metastasis with resection, intracavity carmustine polymer wafers, and radiation therapy is safe and provides excellent local control." *Clin. Cancer Res. 13(12);3637–3641.*

Ferreira, M.M.C. and Suto, E. 1992. "Atomic polar tensor transferability and atomic charges in the fluoromethane series CHxF4-x." *J. Phys. Chem*., 96(22); 8844–8849.

Frisch, A., Nielson, A. B. and Holder, A. J. 2000. GAUSSVIEW User Manual, Gaussian Inc.; Pittsburgh, PA.

Frisch, M.J. et al. 2009. GAUSSIAN 09, Revision A.1, Gaussian Inc., Wallingford, CT.

Fukui, K., Yonezawa, T. andShingu, H. 1952. "A Molecular Orbital Theory of Reactivity in Aromatic Hydrocarbons" J. Chem. Phys., 20; 722.

Glendening, E. D., Badenhoop, J. K., Reed, A. E., Carpenter, J. E. and Weinhold, F. 1996. NBO. Version 3.1, Theoretical Chemistry Institute, University of Wisconsin, Madison.

Gunasekaran, S., Balaji, R.A., Kumeresan, S., Anand, G. and Srinivasan, S. 2008. "Experimental and theoretical investigations of spectroscopic properties of N-acetyl-5-methoxytryptamine." *Can. J. Anal. Sci., Spectrosc*. 53;,149-160.

Hassaniet S. M., Bagheri S. and Ghahremani H. 2012. "A theoretical study on the physicochemical and geometrical properties of the five anti-cancer drug using density functional theory for understanding their biological and anti-cancer activities." *scholars Research Library Annals of Biological Research*, 3(5);2393-2398.

Hoffmann, R. 1988. Solids and Surfaces: A Chemist's View of Bonding in Extended Structures, VCH Publishers, New York.

Hohenberg, P. Kohn, and W. 1964. "Inhomogeneous Electron Gas"Phys. Rev. 136, B864–B871.

Hopkins Medicine Magazine - In Spite of All Odds. Hughbanks, T. and Hoffmann, R. 1983. "Chains of Trans-Edge-Sharing Molybdenum Octahedra: Metal-Metal Bonding in Extended Systems" *J. Am. Chem. Soc.,* 105;,3528-3537.

Irikura, K.K. and Thermo, PL. 2002. (National Institute of Standard and Technology, Gaithersburg, MD)

Johnson, E.R., Keinan, S., Mori-Sanchez, P., Contreras-Garcia, J., Cohen, A.J. and Yang, W. 2010. "Revealing Noncovalent Interactions" *J.Am .Chem. Soc., 132(18); 6498-6506.*

Karabacak, M. and Kurt, M. 2008. "Comparison of experimental and density functional study on the molecular structure, infrared and Raman spectra and vibrational assignments of 6-chloronicotinic acid."Spectrochim. *Acta.,* A 71; 876–883.

Kleimman, D. A. 1962. "Nonlinear Dielectric Polarization in Optical Media."*Phys. Rev*., 126;1977.

Lee, C., Yang, W. and Parr, R.G. 1988. "Development of the Colle-Salvetti correlation-energy formula into a functional of the electron density"*Phys. Rev*., B 37; 785–789.

Li-Jiao Zhao, Xin-yan Ma, Ru-Gang Zhang. 2013. "A density functional theory investigation on the formation mechanisms of DNA interstrand crosslinks induced by chloroethylnitrosoureas*"Internationational journal of quatnaum chemistry, 113,12 99-1306.*

Małecki, J.G. 2010. "Synthesis, crystal, molecular and electronic structures of thiocyanate ruthenium complexes with pyridine and its derivatives as ligands"Polyhedron 29(8);1973-1979.

Martin, J.M.L., Van Alsenoy, C. and Gar2ped.1995. A Program to Obtain a Potential Energy Distribution from a Gaussian Archive Record, University of Antwerp, Belgium.

Murray, J.S. and Sen, K. 1996. Molecular Electrostatic Potentials, Concepts and Applications, Elsevier, Amsterdam.

O'Boyle, N.M., Tenderholt, A.L. and Langner, K.M. 2008. "cclib: a library for package-independent computational chemistry algorithms." *J. Comp. Chem.*, 29(5);839–845.

Parr, R.G. and Chattaraj, P.K. 1991. "Principle of maximum hardness" J. Am. Chem. Soc. 113(5); 1854-1855.

Parr, R.G. and Pearson, R.G. 1983. "Absolute hardness: companion parameter to absolute electronegativity" *J. Am. Chem. Soc.*,105(26);7512-7526.

Parr, R.G., Donnelly, R.A., Ley, M. and Palke, W.E. 1978. "Electronegativity: The density functional viewpoint" *J. Am. Chem. Soc.* 68; 3801.

Parr, R.G., Szentpaly, L.V. and Liu, S.J. 1999. "Electrophilicity Index"*J. Am. Chem. Soc.,* 121(9);1922-1924.

Prabaharan, A. and Xavier, J. J. 2015. "Spectroscopic Aspects, Structural Elucidation, Vibrational and Electronic Investigations of 2-Methoxy-1, 3-Dioxolane: An Interpretation Based on DFT and QTAIM Approach"*Theor. Comput. Sci,* 2(138);2.

Rastogi, V.K., Palafox, M.A., Mittal, L., Peica, N., Kiefer, W., Lang, K. and Ohja, P. 2007. "FTIR and FT-Raman spectra and density functional computations of the vibrational spectra, molecular geometry and atomic charges of the biomolecule: 5-bromouracil"*J.Raman Spectrosc*., 38:1227–1241.

Rozas, I., Alkorta, I. and J. Elguero. 2000. "Behavior of Ylides Containing N, O, and C Atoms as Hydrogen Bond Acceptors"*J. Am. Chem. Soc.,* 122(45);11154-11161.

Scrocco, E., Tomasi, J. 1978. in: P. Lowdin (Ed.), Advances in Quantum Chemistry,Academic Press, New York.

Sundaraganesan, N., Ilakiamani, S., Salem, H. Wojciechowski, P.M. and Michalska, D. 2005. "FT-Raman and FT-IR spectra, vibrational assignments and density functional studies of 5-bromo-2-nitropyridine"Spectrochim*. Acta.,* A 61;2995–3001.

****